MS-1

GPO PRICE $ ______

CFSTI PRICE(S) $ ______

Hard copy (HC) $3.00

Microfiche (MF) .75

ff 653 July 65

[redacted]

N66 29331 (ACCESSION NUMBER)

(THRU)

63 (PAGES)

1 (CODE)

CR-63521 (NASA CR OR TMX OR AD NUMBER)

14 (CATEGORY)

FACILITY FORM 602

THE Bendix CORPORATION

[redacted]

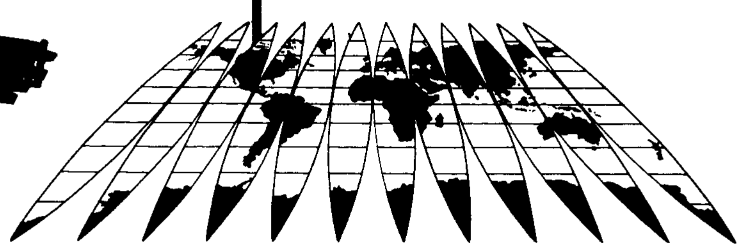

PIONEER-CENTRAL DIVISION

DAVENPORT, IOWA

DEVELOPMENT OF
A PROTOTYPE LH_2
CAPACITANCE TYPE MASS
FLOWMETER AND READOUT

[redacted]

Pub. No. 3170-65
February 22, 1965

THE BENDIX CORPORATION
PIONEER-CENTRAL DIVISION
DAVENPORT, IOWA

Prepared For

GEORGE C. MARSHALL SPACE FLIGHT CENTER
HUNTSVILLE, ALABAMA

Purpose

The Design, Construction and Testing of a Prototype Model of an LH_2 Capacitance Type Flowmeter and Electronic Readout

SUMMARY REPORT

CONTRACT NUMBER NAS 8-5218
REQUEST NUMBER TP3-84022

Prepared By Thomas A. Loftus
Project Engineer

Reviewed By [signature]
Executive Engineer

Approved By [signature]
Chief Engineer

February 22, 1965
Pub. No. 3170-65

TABLE OF CONTENTS

TABLE OF FIGURES

INTRODUCTION

Object of the Report

This report in accordance with the stated content of the summary report, provides a summary of the technical findings, conclusions and recommendations made in connection with Contract No. NAS 8-5218, Request Number TP3-84022. It also includes design principles, procedures, and methods of calculation that will aid in the future development of a capacitive-type mass flowmeter.

Abstract

A capacitive-type mass flowmeter, together with an electronic readout, was designed and built for use with LH_2. Preliminary LH_2 flow tests up to 2 lbs/sec. of LH_2 were conducted at NASA-Huntsville. This test indicated that the force range of the flow sensor was adequate, force nulling or balancing of screen drag forces was being accomplished by the electronic readout, and the system was repeatable. The accuracy of the flow stand was not high enough to permit an accuracy analysis of the Bendix system.

On the basis of the Bendix flowmeter system performance at NASA-Huntsville, a 15 pt. calibration test was scheduled at Wyle Labs., Norco facility. This test was inconclusive because of foreign material in the flow line causing damage to the density sensor and added erroneous drag forces to the force transducers. The existence of an unstable force null (with no flow) was also thought to exist during these tests and to contribute to the scatter of the Bendix rate of flow signal. Extreme difficulty in force nulling was experienced due to the inability of the flow stand to give a no-flow condition of LH_2 at the force sensor for longer than ten seconds. An analysis of the Bendix rate output showed about a $\pm$ 1% of 15 lbs/sec. scatter in the data. This analysis though was inconclusive as only six good data points were available.

As a result of the incurred density sensor damage and the consequent lack of good output data, a second series of LH_2 flow tests were scheduled at Wyle Labs., Norco facility. In addition, a series of nulling stability tests were scheduled at Bendix, Pioneer-Central Division. The latter tests were performed to develop a force nulling technique at LH_2 temperatures.

The Bendix null study indicated that a null instability was present below LN_2 temperatures. This instability occurred with reverse flows or forces, thus it was thought that by keeping a forward force on the flow sensor with the force magnets, this null problem could be circumvented. The Wyle flow tests were then scheduled.

After the flow sensor was stabilized at LH_2 temperatures, a 15 point calibration run was performed. An analysis of the rate-of-flow data indicated that a $\pm$ 2% of full scale scatter was

present in the Bendix rate-of-flow output. This data was then found to be correlated by two straight parallel lines, with a scatter of ± 1% of 15 lbs/sec. about each line. On the basis of a two line correlation indicative of a system having two mechanical null points, the flow sensor was modified to remove the problem. A second series of recorded flows was then conducted. Preliminary runs during cool-down indicated a marked improvement in null stability. The output rate data though seemed to show about the same order of scatter (± 2% of full scale) and correlation as the first series. It was noted during this second series of runs that the vacuum supplied by Wyle surrounding the flowmeter was extremely poor. The tests were then concluded due to the apparent lack of improvement in the rate output after the force sensor modification. Subsequent static tests at Bendix indicated that the second series of rate data should have showed less scatter than the first series. The lack of improvement was attributed to the poor vacuum surrounding the flowmeter and a portion of the transfer line. This poor vacuum caused flow to occur while the force null was being observed, preventing accurate null determination and setting.

Disposition of System

The system is being held at Pioneer-Central awaiting disposition instructions from Marshall Space Flight Center.

Conclusions

The good correlation of the Bendix Indicated Mass Rate of Flow test data from the 15 point calibration on 1-29-65 showing a rate scatter of ≤1% of full scale (15 lbs/sec.) about each of two data correlations shows that the basic theory of operation of the flowmeter system is sound. The fact that two straight lines best correlate the rate data, and the $\sqrt{\text{force}}$ data during nearly constant density runs indicates that some mechanical instability is present. (Post-Wyle static tests show that no magnetic hysteresis or shifts will occur at LH_2 temperatures.)

The mass rate data of 1-29-65 indicates the electronic readout was adequate for the design goal of a mass rate of flow accuracy ± 1% of full scale.

Recommendations

Modification of the force transducer to achieve a softer mechanical null is necessary to obtain a mass rate of flow accuracy of ± 1% of full scale from the Bendix Capacitance Type Mass Flowmeter System.

THE DESIGN, CONSTRUCTION AND TESTING OF A PROTOTYPE MODEL OF AN LH_2 CAPACITANCE TYPE MASS FLOWMETER AND ELECTRONIC READOUT

SCOPE OF WORK

This is quoted directly from Contract NAS8-5218. Our comments to this scope of work as contained in "Proposal for an Improved Cryogenic Mass Flowmeter," Bendix P&QR No. 3123, Pub. No. 2483-62, November 7, 1962, follow. This proposal was in response to RFQ No. TP-3-84022, dated October 25, 1962, for this Capacitance Type LH_2 Mass Flowmeter and associated readout. Since the testing phase was extended, our understanding of these additional tests are also included for clarification.

As quoted from Contract NAS8-5218:

1. Scope and Objective:

   The Contractor, as an independent Contractor and not as an Agent for the Government, shall furnish all of the necessary personnel, facilities and materials (except as may otherwise be provided) and otherwise do all things necessary for or incidental to the performance of the work described below, in designing, building and delivering to Marshall Space Flight Center, a prototype model of a liquid hydrogen capacitance-type mass flowmeter, together with its associated readout for the Liquid Hydrogen Technology Program.

2. Work Statement:

   The Contractor shall design, build and deliver to MSFC a prototype model of a Liquid Hydrogen (LH_2) capacitance type mass flowmeter, together with its associated readout. The mass flowmeter system shall have an overall system accuracy of $\not< 1\%$ when used with cryogenic fluids. The mass flow system shall be capable of measuring flows up to fifteen (15) pounds per second of LH_2.

   a. Construction of the Mass Flow Sensor:

      The mass flow sensor shall be of stainless steel and such other materials that are compatible with Liquid Oxygen (LOX), Liquid Nitrogen (LN_2), and Liquid Hydrogen (LH_2), and will not rust nor corrode in water. The mass flow sensor shall have an inside diameter of three inches (3"). A permanently evacuated, vacuum jacket, shall surround the meter portion. The end fittings shall be four inch (4") one hundred fifty (150) pound ASA stainless steel flanges.

   b. The Electronic Mass Flow Indicator:

      The Electronic Mass Flow Indicator shall be capable of reading the true mass flow when located two hundred (200) to three hundred (300) feet from the flow sensor. The electronic indicator shall provide an analog voltage proportional to mass flow rate suitable for recording on a strip chart recorder. The readout system shall also be capable of totalizing the mass flow through the meter. This information shall be in engineering units or in such form as to be easily converted to engineering units such as total pounds or total kilograms.

This equipment shall operate on 110 volts AC or 28 volts DC.

Comments to Scope of Work Document

Review of the "scope-of-work" reveals that explanation or clarification of a few items is necessary so that both NASA and contractor personnel have a clear understanding of the requirements.

Article I - Scope of Work

2. Work Statement

"The mass flowmeter system shall have an overall accuracy of $\pm$ 1% when used with cryogenic fluids."

Pioneer-Central interpretation of this requirement is that the mass rate of flow accuracy requirement allows for a 1% error in measurement of the full scale range at any flow rate up to the rated capacity. This is a standard instrument allowable error requirement.

As the proposed design approach is for a flowmeter to handle liquid hydrogen and utilizes a physical principle of the relationship of dielectric constant to density for non-polar fluids, it should be understood that the terminology of "cryogenic fluids" means, in this case, only liquid hydrogen and liquid nitrogen. Such "cryogenic fluids" as liquid fluorine, methane, etc., shall not apply to the requirement.

Article I - Scope of Work

2. Work Statement

"The mass flow system shall be capable of measuring flows up to fifteen (15) pounds per second of LH_2."

Pioneer-Central interpretation of this requirement is that the design shall be capable of measurement of a maximum flow rate of 15 lbs/sec. of LH_2. Pioneer-Central will design the flowmeter for a dynamic flow range of 10:1 hence, the actual measurement range shall be from 1.5 lbs/sec. to 15 lbs/sec. of LH_2.

ADDITIONAL TESTS ON PIONEER-CENTRAL LIQUID HYDROGEN FLOWMETER WHICH ARE BEYOND THE SCOPE OF PRESENT MSFC FORMAL TEST REQUIREMENTS

1. With the Pioneer-Central liquid hydrogen flowmeter installed in test stand, slowly flow LH_2 through the unit for a minimum of 2-1/2 hours to assure proper cool down. Conduct a series of recorded flow tests (up to 24) at the approximate rates to be specified by Pioneer-Central engineers present during the tests. Such flow rates will be between 1.5 and 15 pounds per second and are for the purpose of establishing the optimum nulling and calibration techniques.

   A check on the null setting will be required at intervals during these tests. A minimum of three recorded flow tests at widely separated rates will be needed between null setting checks to determine if any change has taken place. Each null check will require a static condition (cold gas or quiescent liquid) at 45 to 50 psia in flowmeter at LH_2 temperature for at least ten seconds.

   The usual standard test equipment will be required, including recorders as follows:

   > Three channels on strip chart recorders having 12 inch or more total deflection. Total accuracy and linearity of 0.5% is required from 10% to 100% of full scale reading. Two of the channels to be adjustable from 20 mv. to 100 mv. for full scale deflection. Third channel to be offset such that full deflection occurs when input signal changes from 50 mv. to 100 mv.

   When the above tests are completed, the vacuum chamber surrounding the flowmeter should be opened and purged with dry gas over night to permit the flowmeter to warm to ambient temperature.

2. With unit near ambient temperature, remove flowmeter for inspection, reinstall, and prepare stand for testing. Bring flowmeter down to LH_2 temperature by slowly flowing liquid through unit for at least 2-1/2 hours. Conduct up to six recorded flows at approximate rates to be specified by Pioneer-Central engineers. The null should be checked at intervals in accordance with the procedure noted in item 1.

   With system operating properly, proceed with the formal calibration test for the George Marshall Space Flight Center. If and when a malfunction is noted, it is requested that a test at the same flow rate be repeated. If the malfunction continues, the flowmeter should be allowed to warm to a temperature above the dew point, removed, and inspected by Wyle and Pioneer-Central personnel to establish the cause. Removal prior to warming up above dew point will cause wetting of the internal points and cause further delays to thoroughly dry the unit. Any correction necessary to flowmeter or test stand indicated by a malfunction should be by mutual agreement between Wyle personnel and Pioneer-Central engineers. Any data taken during the period when the operating conditions are other than normal should be voided or an explanation included with the data.

3. The two phase flow tests described below should be treated separately from those above, since they may or may not be performed. If conducted, they should be scheduled so as to not interfere with the tests given above.

   Conduct two phase flow test using some of the same rates of flow as used in single phase flow tests previously described. Such tests should include flow rates spread over as much of the 1.5 to 15 lbs. per second range as possible. Single phase and two phase test results for each rate of flow used should be compared to determine effect on flowmeter.

   It is requested that the two approaches given below be considered:

   (a) Inject warm helium or hydrogen gas at various rates into the LH_2 flow stream and check the effect on the flowmeter. Repeatability of the flowmeter readings under various conditions should be established.

   (b) Inject cold helium or hydrogen gas of known quantities and rates and determine accuracy and repeatability of the flowmeter under given two phase flow conditions.

FLUID MEASUREMENTS REQUIRED

In order to meet the demands for fast response and extended operation at cryogenic temperatures, Bendix Pioneer-Central Division, under contract with NASA-Huntsville, constructed a prototype LH_2 mass flowmeter system. The system shown in Figure 1 measures flow rate by making two separate measurements on the fluid passing through a pipe.

(1) Density of the fluid.
(2) Integrated drag force the fluid exerts upon a wire screen placed in the flow stream.

These separate analogs are multiplied together to obtain an analog of mass flow rate. This analog is later integrated with time to obtain a total flow indication. The attractive features of these system elements are that they:

(1) Are theoretically unaffected by two phase flow.
(2) Require only microseconds to detect null errors.
(3) Permit elimination of friction bearings allowing more accurate drag force measurements and long term unattended operation at cryogenic temperatures.
(4) Are not subject to overspeed.
(5) Are not subject to fatigue failure.

The transducer or flow detecting element also incorporates a counter-balance so that the transducer should to a large degree be insensitive to the intensity, frequency or orientation of body acceleration forces. As originally designed, this prototype was intended for study and environmental tests to prove a theory and our mechanical and electrical design concepts.

The principles upon which the flow sensor operation is based are well founded and have been proven by numerous experiments. The pressure drop across a round wire screen in the form of a square-mesh lattice was investigated by W. D. Baines and E. G. Peterson, "An Investigation of Flow Through Screens," TRANS. ASME, July, 1951, pp. 467-480. They found that irrespective of the flow velocity profile, that the pressure drop ΔP across a screen of a given form and solidity ratio was proportional to the rate of energy loss of the flow across this screen. In terms of flow parameters,

$$\frac{\Delta P}{\rho V_o^2/2} = K$$

where:

ΔP = local pressure drop (at screen)
ρ = mass density averaged over the screen
V_o = spatial mean velocity
K = pressure drop coefficient

For a given screen form and solidity ratio, and above a screen Reynold's number,

$$R = V_o \, b/\nu$$

where:

b = bar width
ν = dynamic viscosity μ/mass density ρ, $= \mu/\rho$

at 10^3, no variation of K with R was observed. Thus the drag force $\Delta P \, A_t$ (where A_t = total screen area) of the fluid on the wire screen is related to ρV_o^2 by an unvarying constant above $R = 10^3$. The expression desired though is the mass rate of flow through the wire screen or,

$$M = \rho V_o \text{ lbs. sec.}^{-1}\text{ft.}^{-2}$$

Thus by employing a trip balance scheme, we balance the screen drag force F with end attracting electromagnets. Measuring the balancing current (at a constant known magnet gap) where $F \propto I^2$, the electromagnet current can be related to the screen drag as,

$$I \propto V_o \sqrt{\rho}$$

Since ρ and V_o are independent variables, a measure of ρ must now be obtained.

It is known that for cryogenic fluids the dielectric constant ϵ of the medium is related to its density ρ by the Clausius-Mossotti relation (with certain restrictions)

$$\frac{\epsilon - 1}{\epsilon + 2} \quad \frac{1}{\rho} = P$$

where P = specific polarization.

By inserting a set of flow-through capacitor plates in the flowstream, and measuring the capacitance change which is proportional to ϵ, a measure of ρ is obtained.

Operating electronically on this signal so as to obtain $\sqrt{\rho}$, the magnet current required for null and the modified capacitor signal may be electronically combined to give an output signal E proportional to mass rate of flow or,

$$E \propto V_o \sqrt{\rho} \cdot \sqrt{\rho}$$

or $\quad E \propto \rho V_o$

Therefore, $E \propto M$ lbs. sec.$^{-1}$ft.$^{-2}$

The mechanical and electrical make-up of the flowmeter system that was needed to obtain this final output signal is discussed in the next section.

Since this LH_2 mass flowmeter is based on operational principles that hold for all non-polar cryogenic fluids, a mass flowmeter system may be designed using these same principles, to operate over different flow ranges for the same fluid and with varying flow ranges for other fluids.

SYSTEM COMPONENTS DEVELOPED

A. Flow and Density Sensors

The present flowmeter prototype (see Figure 1) and photographs has a three (3) inch diameter flow channel and four (4) inch mounting flanges, (Marmon-Aeroquip "Conoseal") at each end for mounting in a three (3) inch line. The housing is one piece stainless steel and the flanges are integral. The enlarged flange is to permit assembly access to the density and force sensors, and to keep their mounting rings out of the main flow channel.

The density sensing plates are of welded stainless steel honeycomb, silver brazed into a stainless steel ring. They are insulated electrically from the housing and each other. Their adjacent honeycomb faces are the plates of a fixed gap capacitor through which fluids may flow. Electrical leads to these plates are through fused glass insulated feed-throughs silver brazed into the housing. There is a set of density plates on each side of the force screen to provide additional active (working) capacitance. The figure shows one set of plates.

The force screen assembly (crossed wires mounted in a ring) assembles to the collector ring. Force on the screen (from flow) is transmitted out of the flow chamber through levers located radially about the collector ring (with lever axis perpendicular to the meter axis). The levers have thin metal discs attached for end and fulcrum pivots. The inner and fulcrum pivot discs provide means of hermetically sealing the lever through the meter wall and are opposed with respect to pressure differential so that internal fluid pressure causes no force along the lever axis. The inner lever pivot mounts to the collector ring.

The outer pivot discs mount to a rigid annular frame that is attached to the outside of the housing through two annular thin metal supports.

Motion is limited to fore and aft parallel to the meter axis and the force screen and annular frame remain perpendicular to that axis. The force screen is one platform and the annular frame the other, of a reversing platform balance. A force anywhere on the face of the screen may be measured in the opposite direction at any point of the face of the frame. The LH_2 drag force on the screen varies from 0.03 to 3.00 lbs. over the 1.5 to 15 lbs/sec. mass rate of flow range.

The active (center) null capacitor plate and the magnet plates are mounted to the annular frame. Each of the null capacitor plates is in three segments that form a flat ring when mounted. The fixed (outer) null plates and the electromagnets are

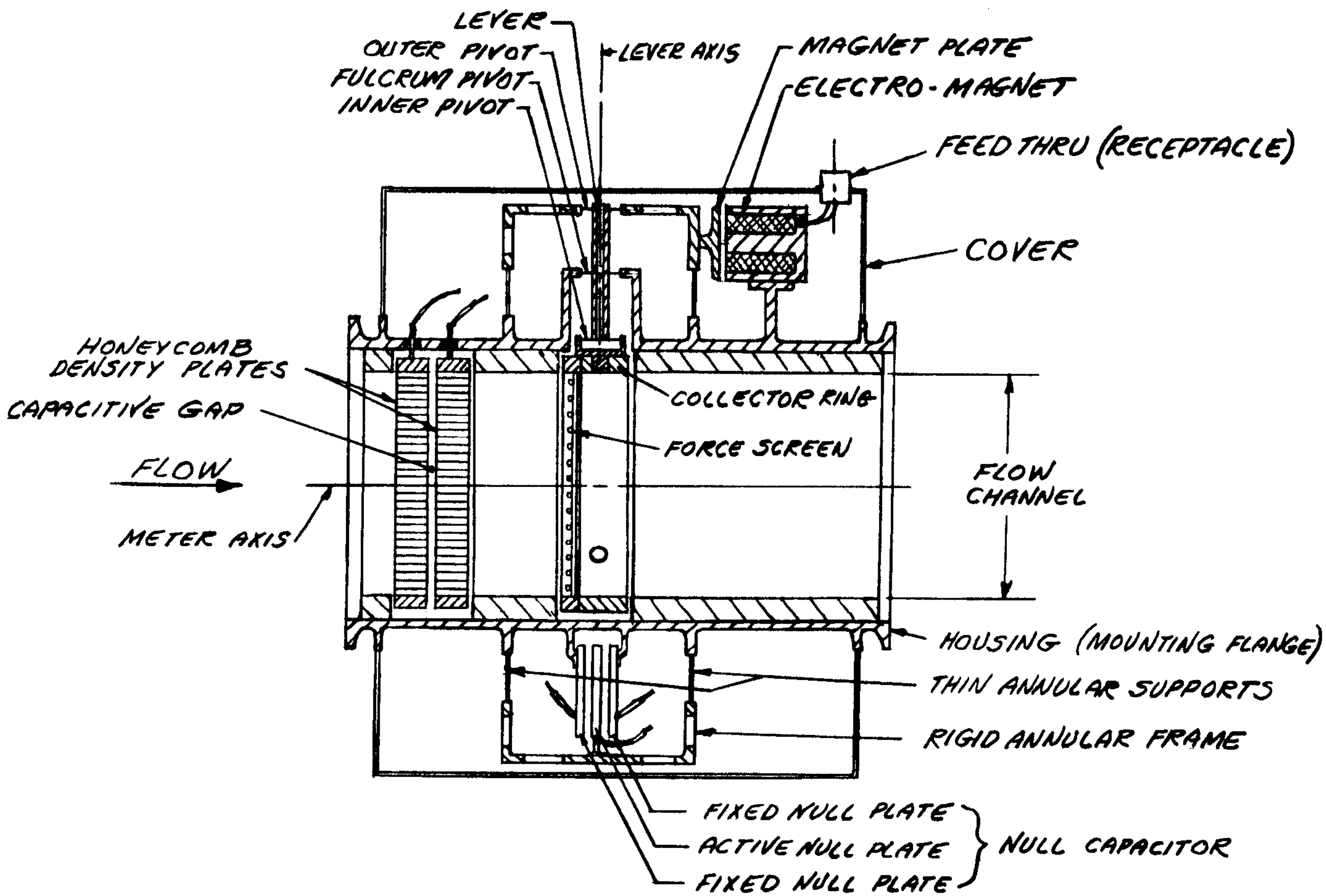

TRANSDUCER SCHEMATIC

B9-41198-4

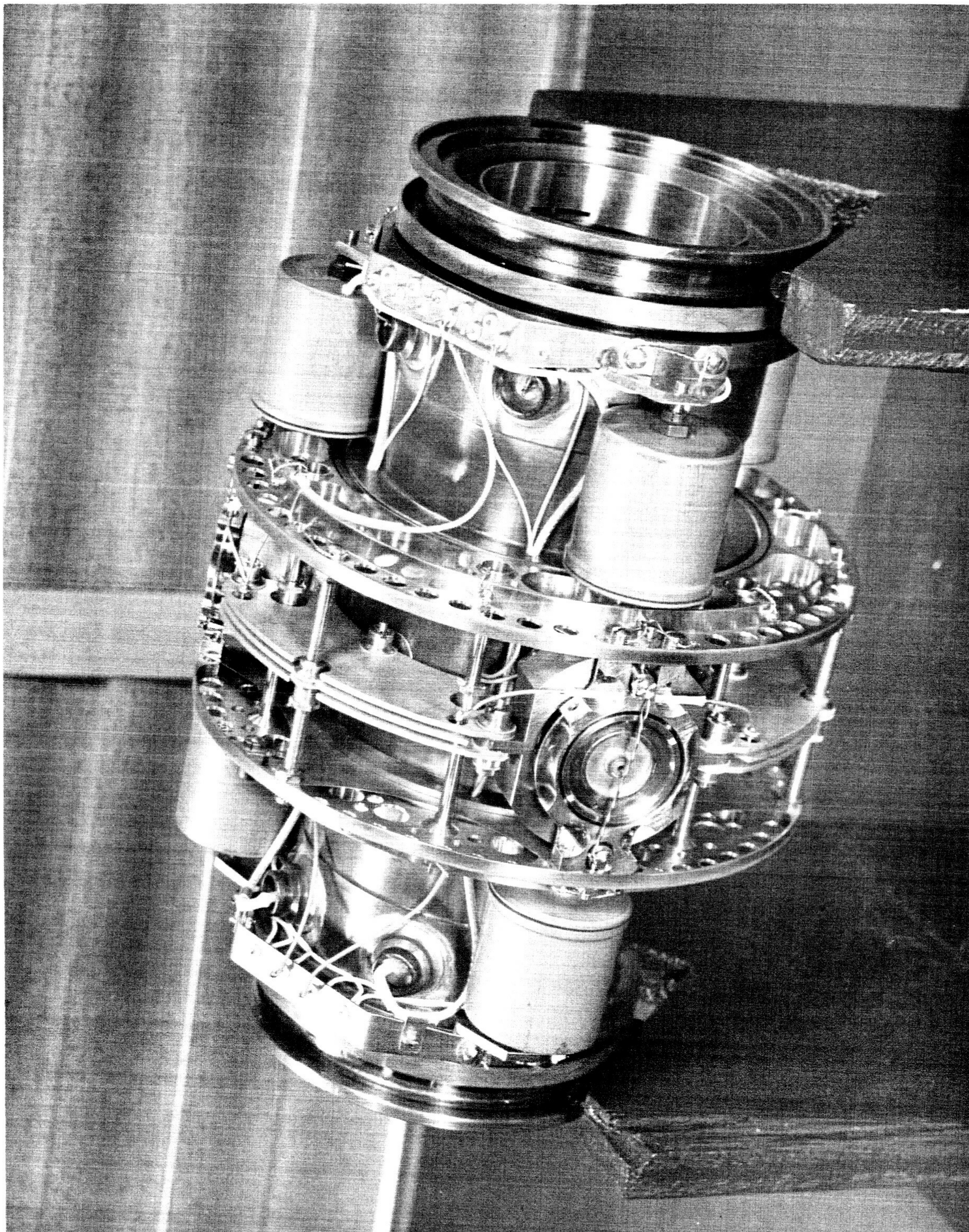

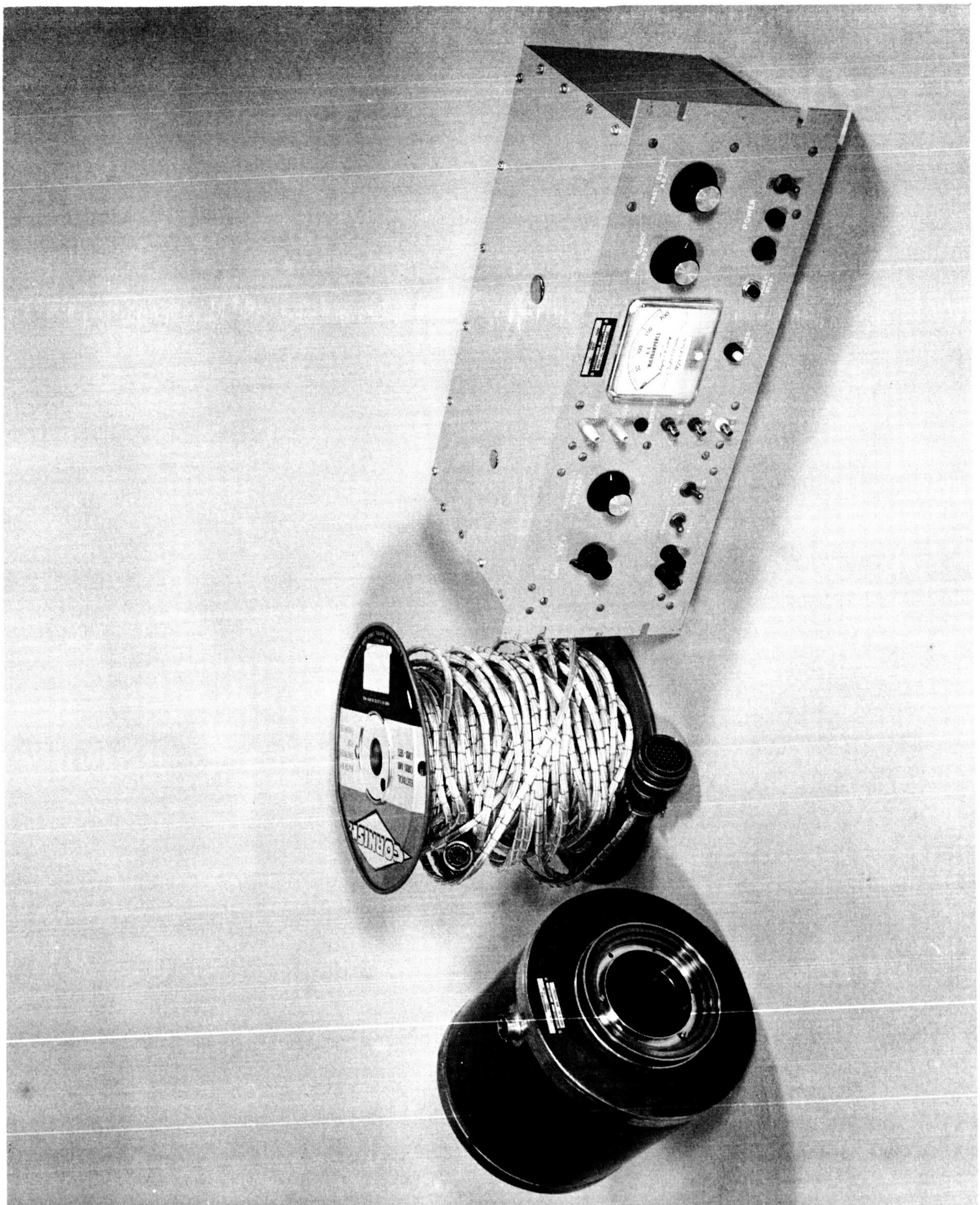

mounted to the meter housing. The three (segmented) null plates are insulated electrically from the housing and each other.

Two way stops at both ends of the levers limit the maximum travel to a few mils to prevent overstress.

The outer parts counterbalance the inner parts through the levers making the system insensitive to position and acceleration force. The prototype has a 2 to 1 lever ratio.

A protective sealed cover permits inert gas back filling for optimum electrical stability and improved heat transfer between the enclosed parts for quicker temperature stabilization.

The prototype has two sets of magnets for measuring forward or reverse flow. By using low magnetic hysteresis, high permeability magnetic materials, these magnets can give forces repeatable to 0.006 lbs. This repeatability is achieved when the magnets are operated over an 0.06 to 6.00 lb. range, necessitated by the 1:2 balance arm ratio.

There are no sliding or rotating parts. The minute amount of travel (sensitivity) required is obtained by the deflection of materials. There are restoring spring forces but these do not affect the measurement function. The mechanical accuracy is dependent on capacitor stability and material hysteresis. Mechanical sensitivity and response time is dependent on the total weight of the force sensing parts and the stiffness of their suspension.

The following graph Figure 2 shows the variation of Reynolds number with mass flow of LH_2 for varying wire grid sizes. A choice of 0.041" diameter wire size was made, which can be seen to be well over the $Re = 10^3$ minimum. From the next graph, Figure 3, we may find the force of the flow on the wire screen over the design flow range. This is the force which must be balanced and hence measured by the electromagnets in the force servo. These forces vary over a 100:1 range when flow varies over a 10:1 range.

Since the density (ρ) versus dielectric constant (ϵ) of hydrogen is known to 0.1% over a theoretically possible operating range of 0 to .08 g/cc (gas to liquid [14°K]), a fit to the data can be made. Using the Clausius-Mossotti correlation (which is accurate to 0.1%) of density vs. dielectric constant, a best straight line fit is made to the dielectric values computed from the Clausius-Mossotti correlation. This fit is shown in the next graph, Figure 4, of density vs. LH_2 dielectric constant. It is calculable that this straight line fits the available data to 0.1% (of ϵ at 0.08 g/cc) over the 0 to 0.08 g/cc density range.

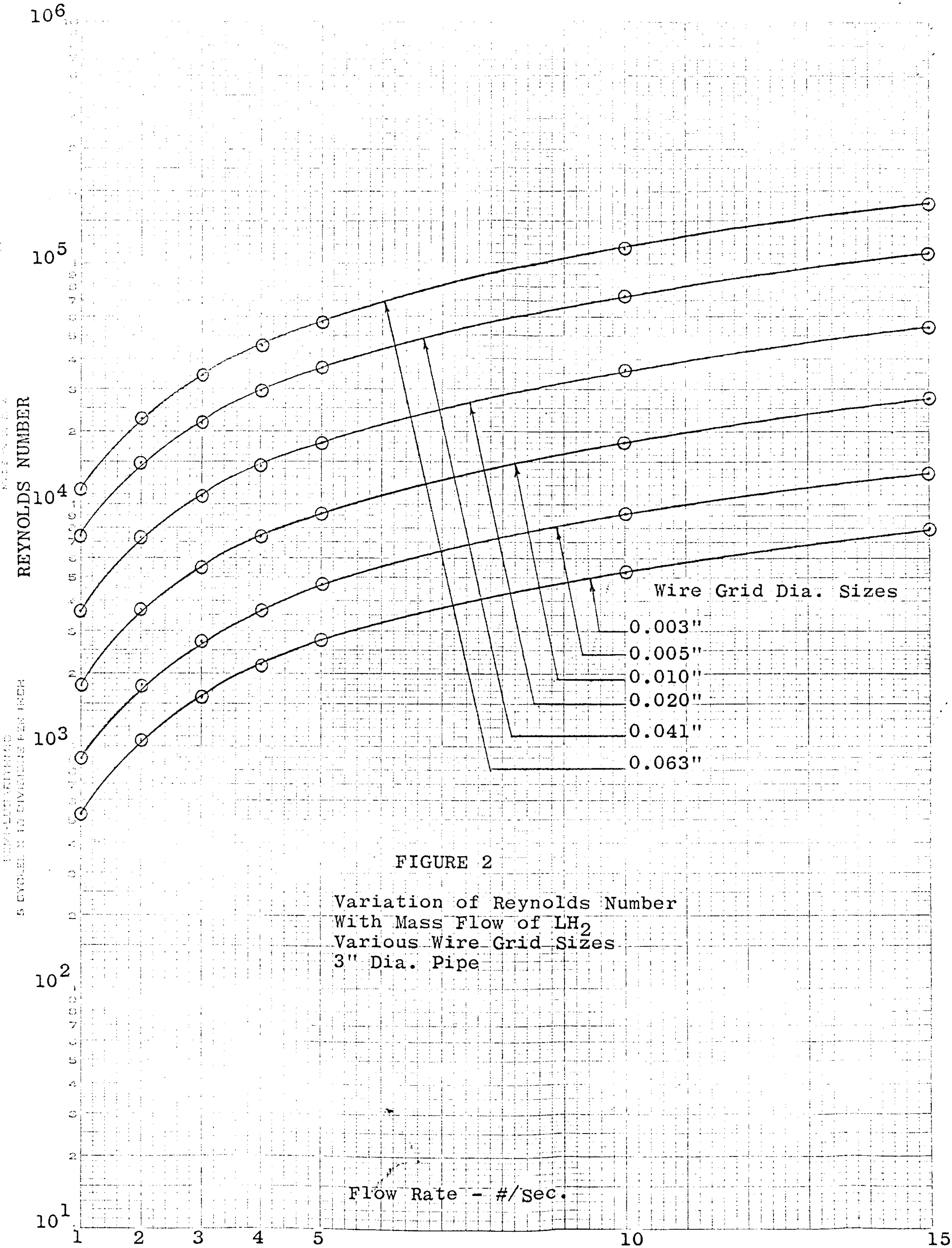

FIGURE 2

Variation of Reynolds Number
With Mass Flow of LH_2
Various Wire Grid Sizes
3" Dia. Pipe

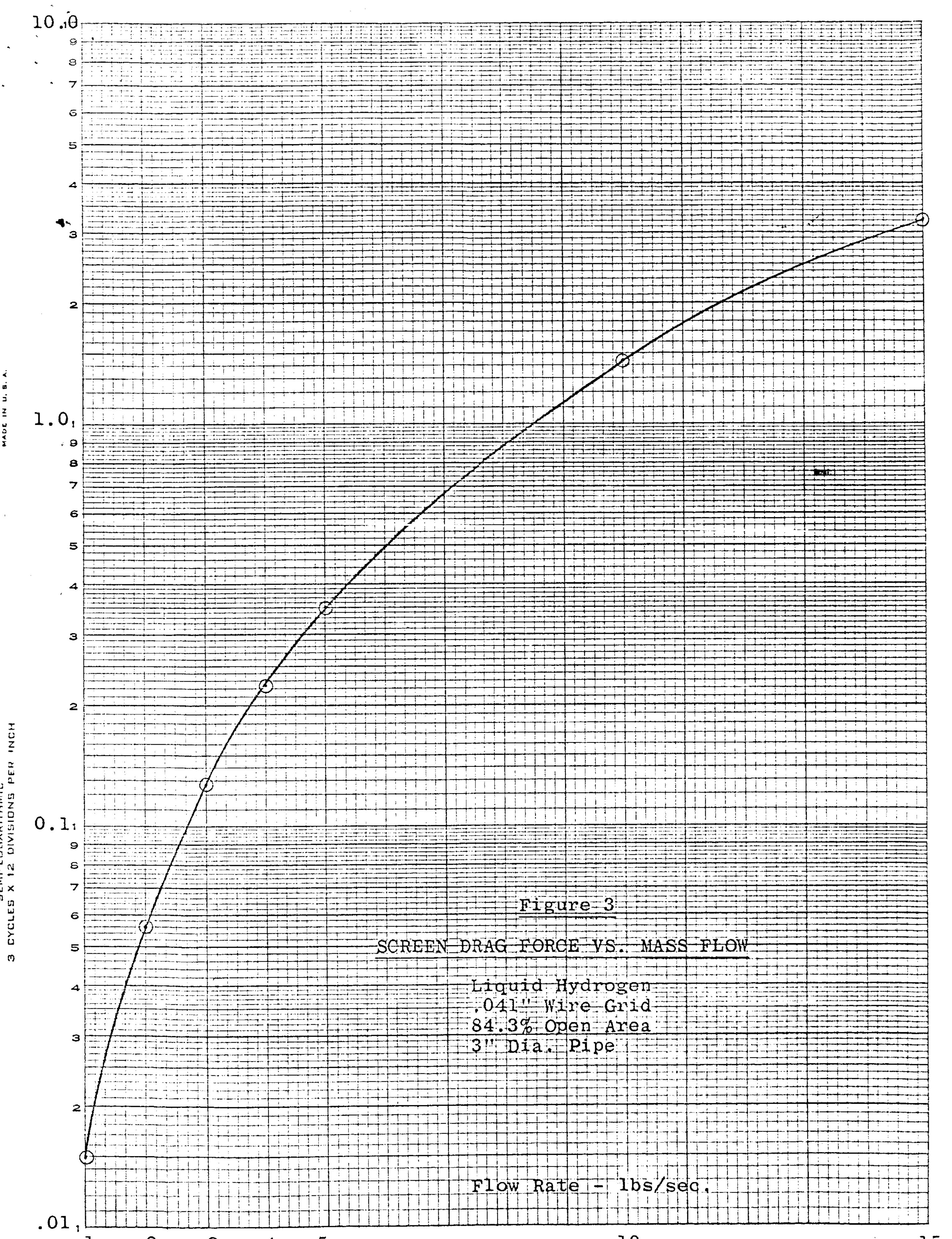

Figure 3

SCREEN DRAG FORCE VS. MASS FLOW

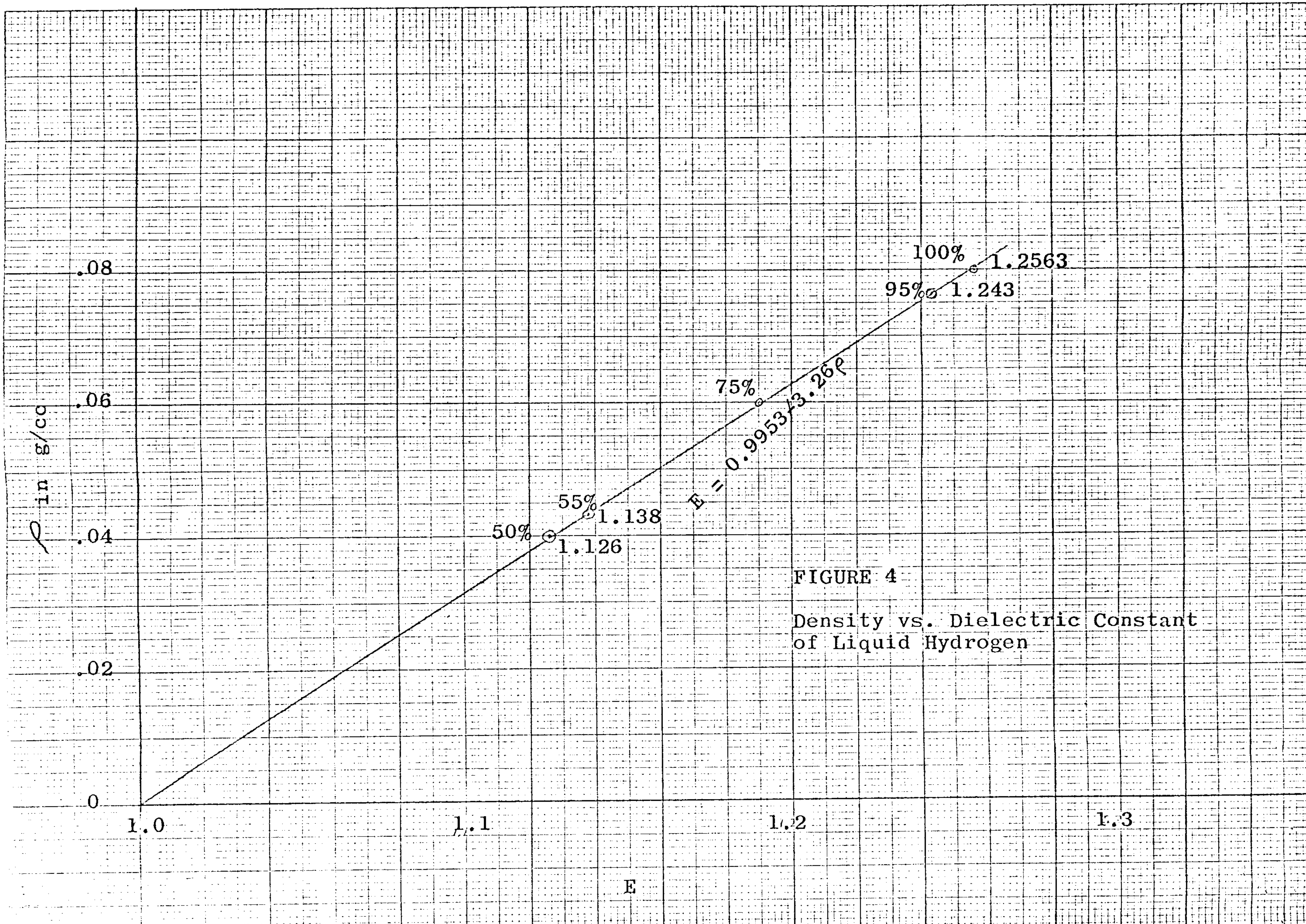

FIGURE 4

Density vs. Dielectric Constant of Liquid Hydrogen

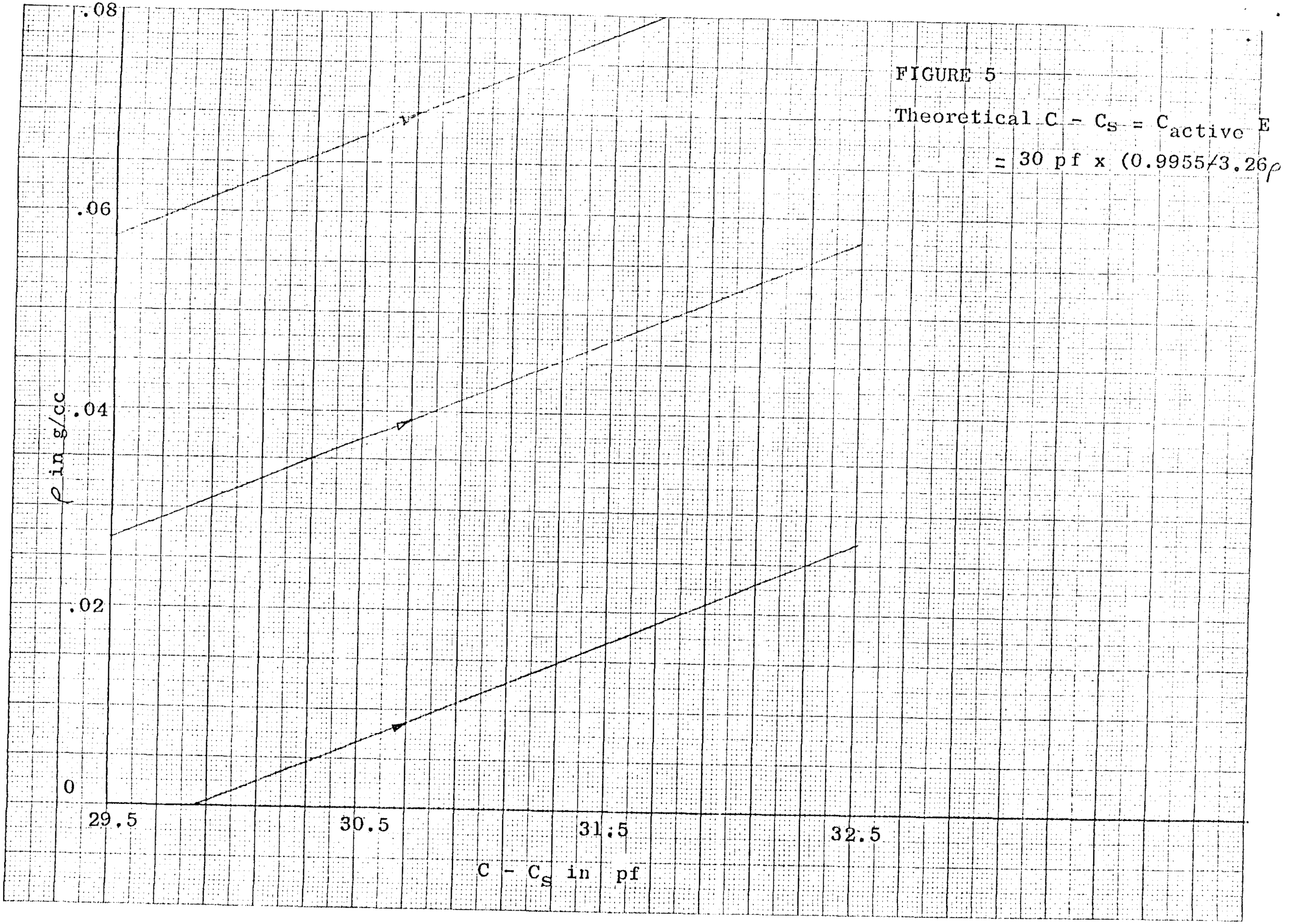
FIGURE 5
Theoretical $C - C_s = C_{active}\ E$
$= 30$ pf x $(0.9955/3.26\rho$
.08
.06
.04
.02
0
ρ in g/cc
29.5
30.5
31.5
32.5
$C - C_s$ in pf

By immersing the density sensing capacitors in several calibrating mediums (GN_2, LN_2), their active and stray capacitance is determined. With the help of the ϵ vs. ρ relation previously obtained, the change in the density sensor capacitance can be found over the operating range. This is shown in Figure 5.

B. Electronics Readout

The density of the flowing material is obtained from its dielectric constant and is measured by two honeycomb plates across the full flow area. The adjacent faces of the honeycombs are the plates of a fixed gap capacitor. This provides the servo with an instantaneous capacitance (density) value.

As previously discussed, the force screen, a crossed wire grid across the full flow area, is supported on a lever system with sealed diaphragms as pivots and fulcrums. The sensitive null capacitor plate is mounted on the outer ends of the levers. The fixed null capacitor plates are mounted to the housing. Any force on the screen caused by flow causes a shift in the null and requires a proportional force from the magnets, mounted also at the outer level ends, to restore it. The servo senses this null shift and instantly provides the required power to the magnets.

The density proportional capacitance and the kinetic energy proportional magnet power is combined electronically and appears as a varying D.C. output voltage that is proportional to mass rate of flow.

The rate flow electronics is shown in Figure 6 in block form with the force servo, the density servo and the multiplier electronics. The density and force servos are blocked out in greater detail in Figures 7 and 8.

The force servo is a phase locked capacitance servo. A digital feedback circuit is incorporated which feeds back an analog staircase to the magnets to apply force to the transducer opposite that applied against the force screen. Relative movement is sensed by the capacitor in the transducers attached to the screen. A sensitive capacitance bridge detects an unbalance of less than ten microinches. This unbalance is converted to a D.C. voltage in the phase null detector. In turn, this commands the staircase generator to increase or decrease in magnitude by reversing a counter from which the staircase is being derived.

Since the minimum change in feedback is one step of the staircase, there is a $\pm$ one count hunt around a null point. There are 1024 integer steps used in the staircase.

This hunting reduces transducer damping problems. An analog of the force output is obtained by measuring the current feedback to the magnets. The force output of these magnets is proportional to the square of the current and, therefore, a voltage is obtained proportional to the square root of force.

$$E_{out} \propto V_o \sqrt{\rho} \propto \sqrt{force}$$

BLOCK DIAGRAM - RATE OF FLOW SYSTEM

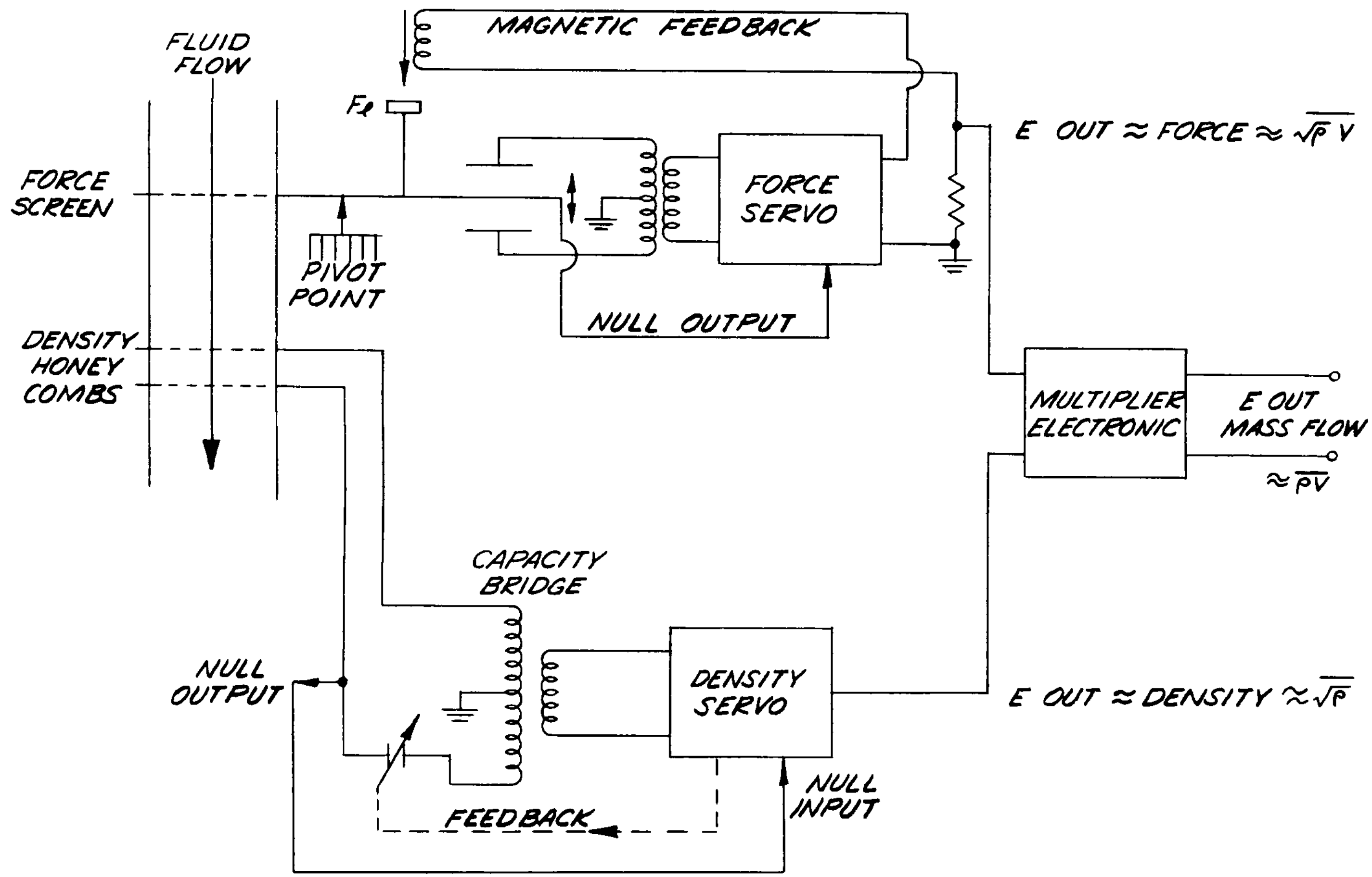

A9-41198-3

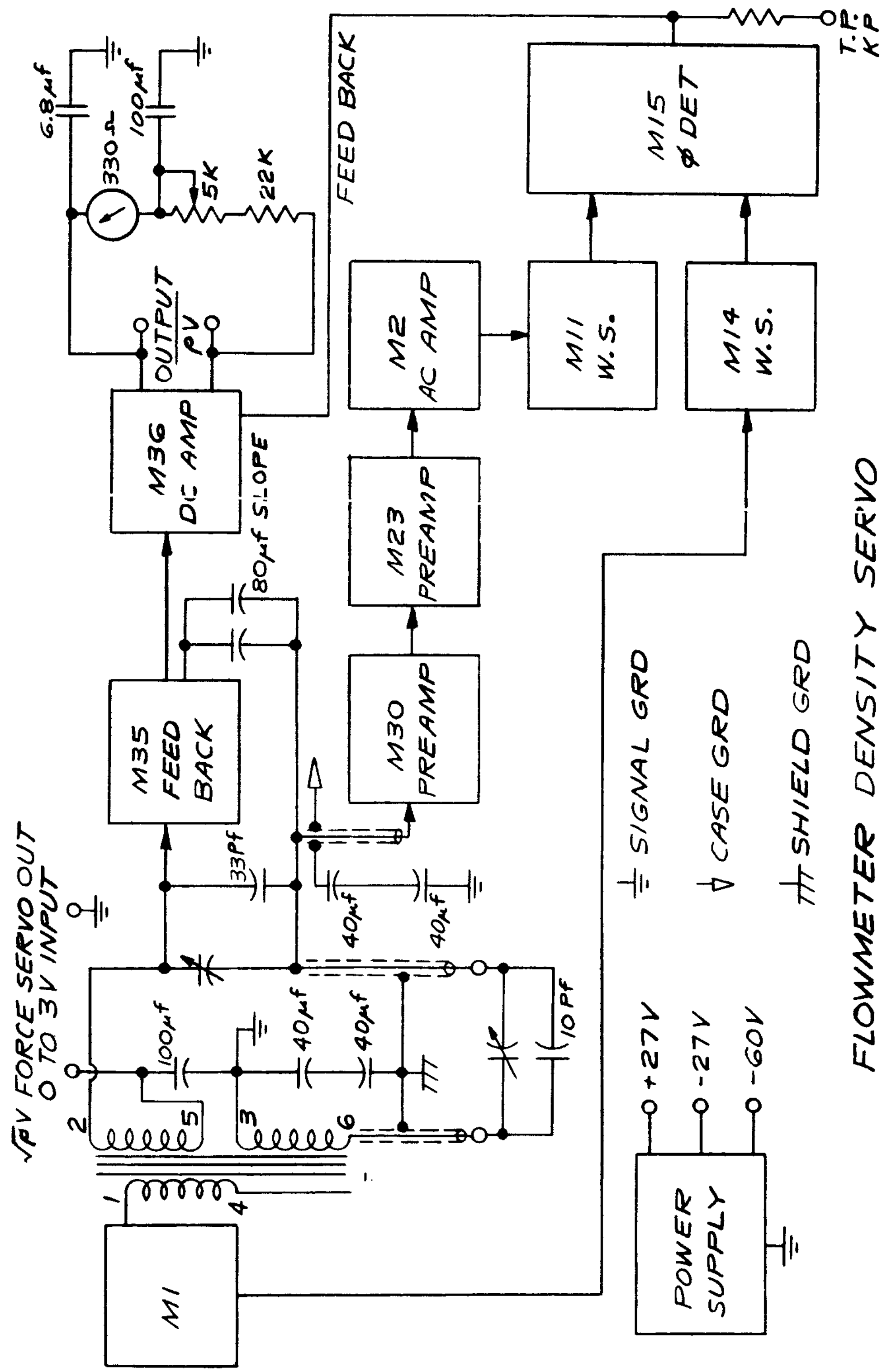

FLOWMETER DENSITY SERVO

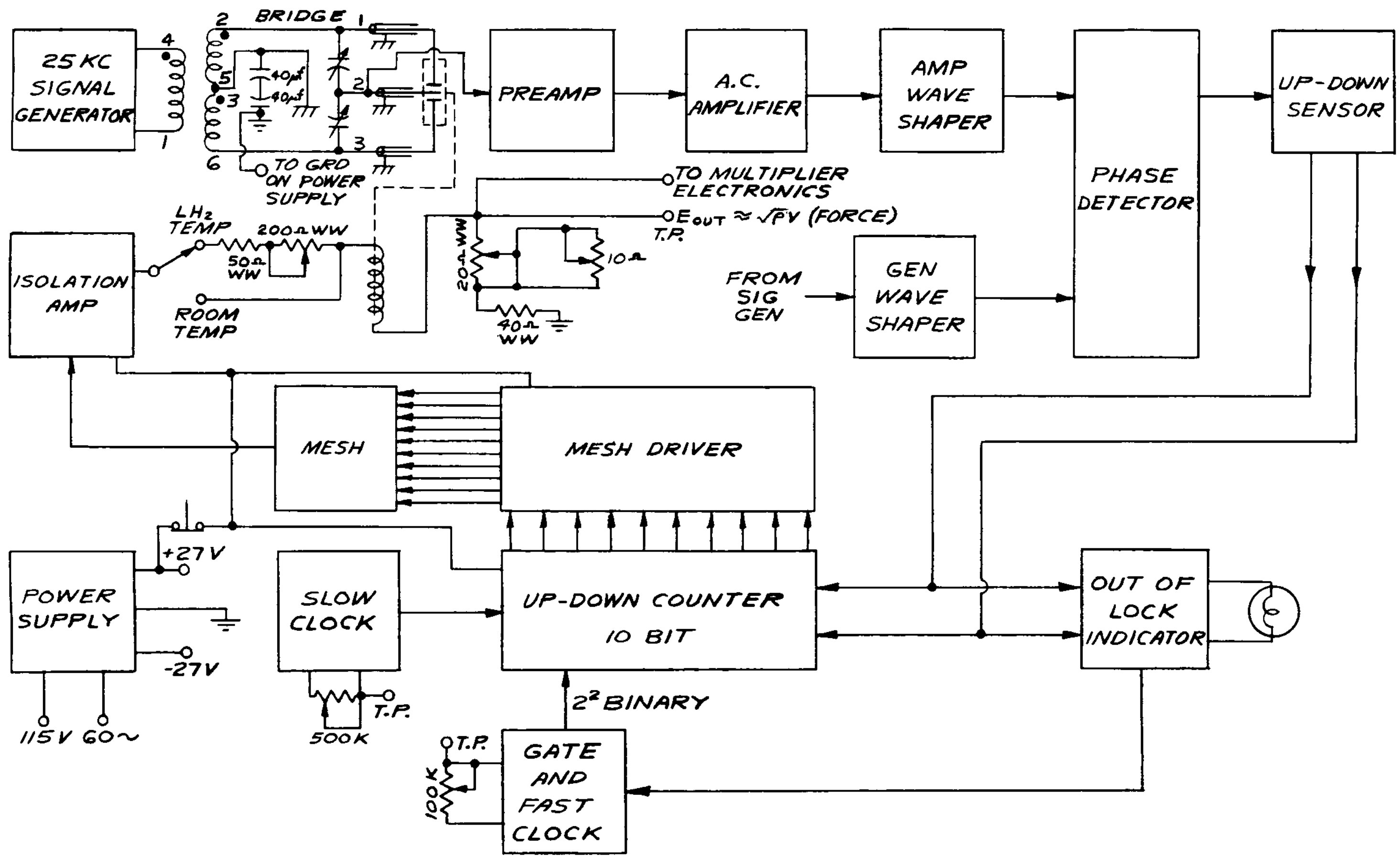

FORCE SERVO

B9-41198-5

This output is later multiplied by the square root of density ($\sqrt{\rho}$) and mass flow rate is obtained.

$$\text{Mass flow rate} = M = \sqrt{\rho}\ (V_o \sqrt{\rho}\ ) = \rho\, V_o$$

The density servo is also a capacitance phase locked servo. In this case, a non-hunting feedback loop is used. A field effect transistor is used as an electronic potentiometer to vary A.C. feedback voltage feed to maintain bridge balance.

A straight line approximation of the square root of density is used to obtain an analog output. This straight line is obtained by adjusting bridge constants. Accuracy is not impaired since the dynamic range of density is relatively small.

The force and density analogs are multiplied together using an electronic equivalent of a motor driven potentiometer. (Driven potentiometers are commonly used in analog computers to multiply.) A field effect transistor is used in a special circuit arrangement to accomplish this result.

The multiplier is included within the closed loop of the density servo, as is all of the circuit. This reduces drift problems.

A totalizer is obtained by making an analog to digital conversion of the rate flow analog. The digital number is sampled at a fixed rate and accumulated in a mechanical counter (See Figure 12).

To give an idea of the manner in which the $\sqrt{\rho}$ is obtained when $E_{out} = K\rho$ and $E_{out} = K\,V\sqrt{\rho}$ are electronically combined, we consider the following graphs.

In Figure 9 we plot ρ vs. $\sqrt{\rho}$ and set the maximum and minimum allowable range of ρ. This now sets the range of $\sqrt{\rho}$. Thus if ρ covers the 100% to 50% of ρ max. range, we make a best straight line fit to ρ vs. $\sqrt{\rho}$. Making the fit through the 55% and 95% of ρ max. points, a change of ρ from 55% ρ max. to 95% ρ max. should change $\sqrt{\rho}$ from 2.1 to 2.75. This is a 65/2.75% = 23.64% change of the $\sqrt{.95\rho}$ max. signal. From the same line, a 100% ρ max. to 50% ρ max. causes a 28.87% in $\sqrt{\rho}$ max. signal. Thus when the $K\rho$ and $K\,V\sqrt{\rho}$ signals are electronically combined, the $K\rho$ signal must effect the $V\rho$ max. signal such that when $K\rho$ goes 100% to 50% ρ max., $V\rho$ goes 100% to 71.13% of $V\rho$ max.

Going back to the graph of C vs. ρ (Figure 5) for the density sensor, the C vs. $E_{out} = K\rho$ is plotted to determine that it is a straight line. This is given by Fig. 10. In Fig. 11 now is a plot of the actual variation of $E_{out} = \rho V$ for a

95% ρ max. to 55% ρ max. change in C or the $K\rho$ signal. As it should be $E_{out} = \overline{\rho V}$ varies by 23.6% as C proportional to ρ varies over the $C \propto 95\%\ \rho$ max. to $C \propto 55\%\ \rho$ max. operating range.

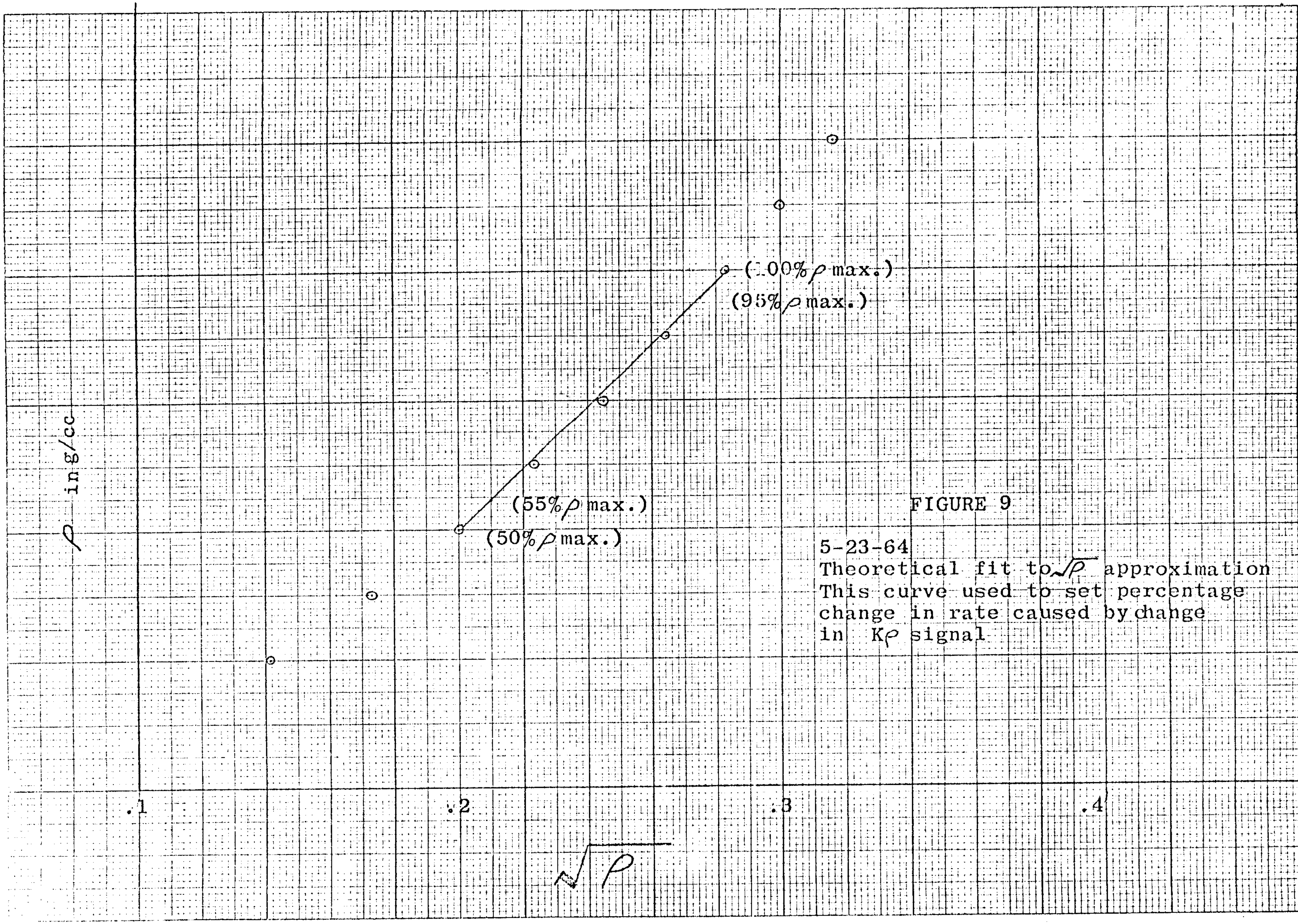

FIGURE 9

5-23-64
Theoretical fit to $\sqrt{\rho}$ approximation
This curve used to set percentage
change in rate caused by change
in $K\rho$ signal

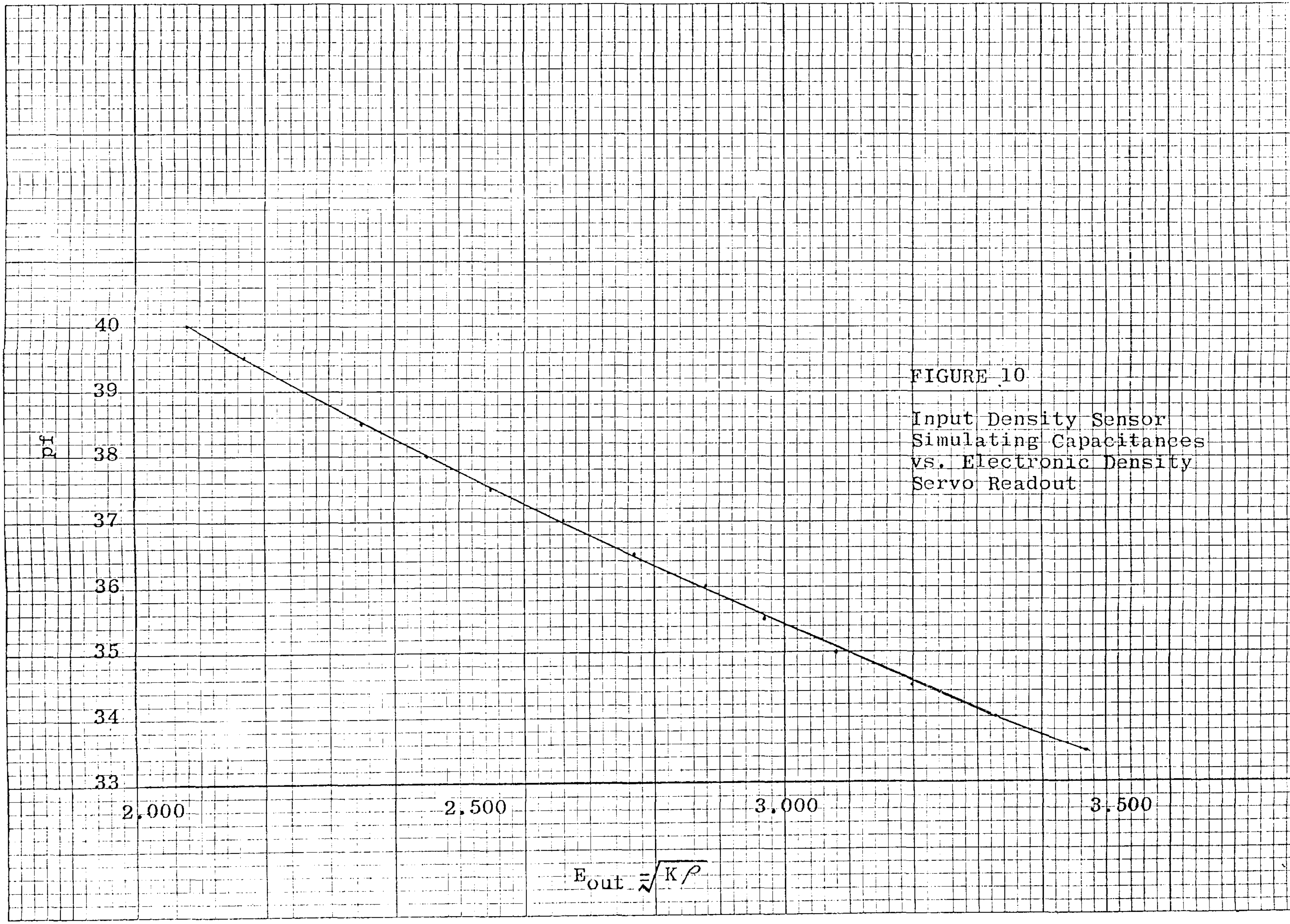

FIGURE 10

Input Density Sensor
Simulating Capacitances
vs. Electronic Density
Servo Readout

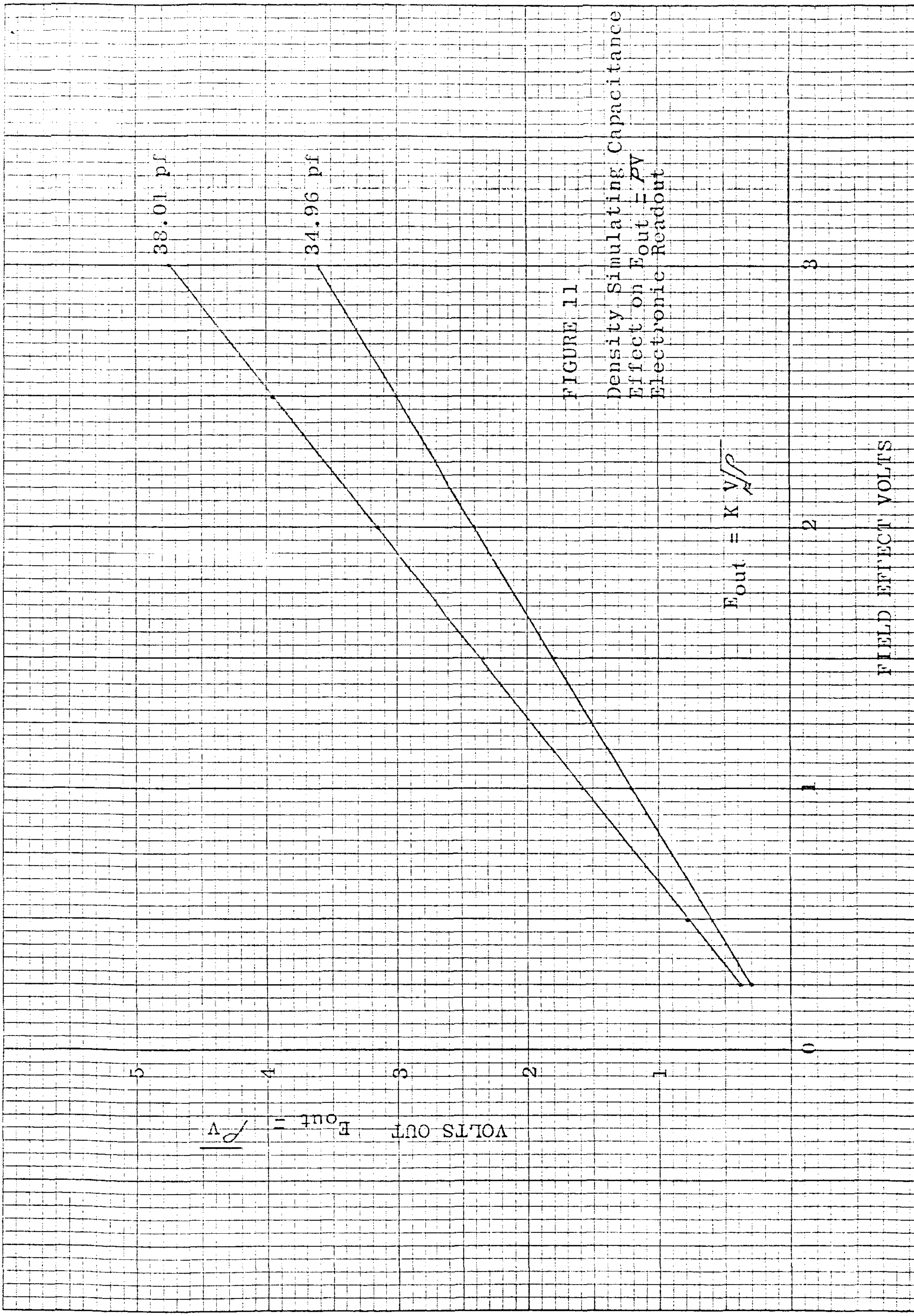

FIGURE 11

Density Simulating Capacitance Effect on $E_{out} = \rho V$ Electronic Readout

FLOW TOTALIZER

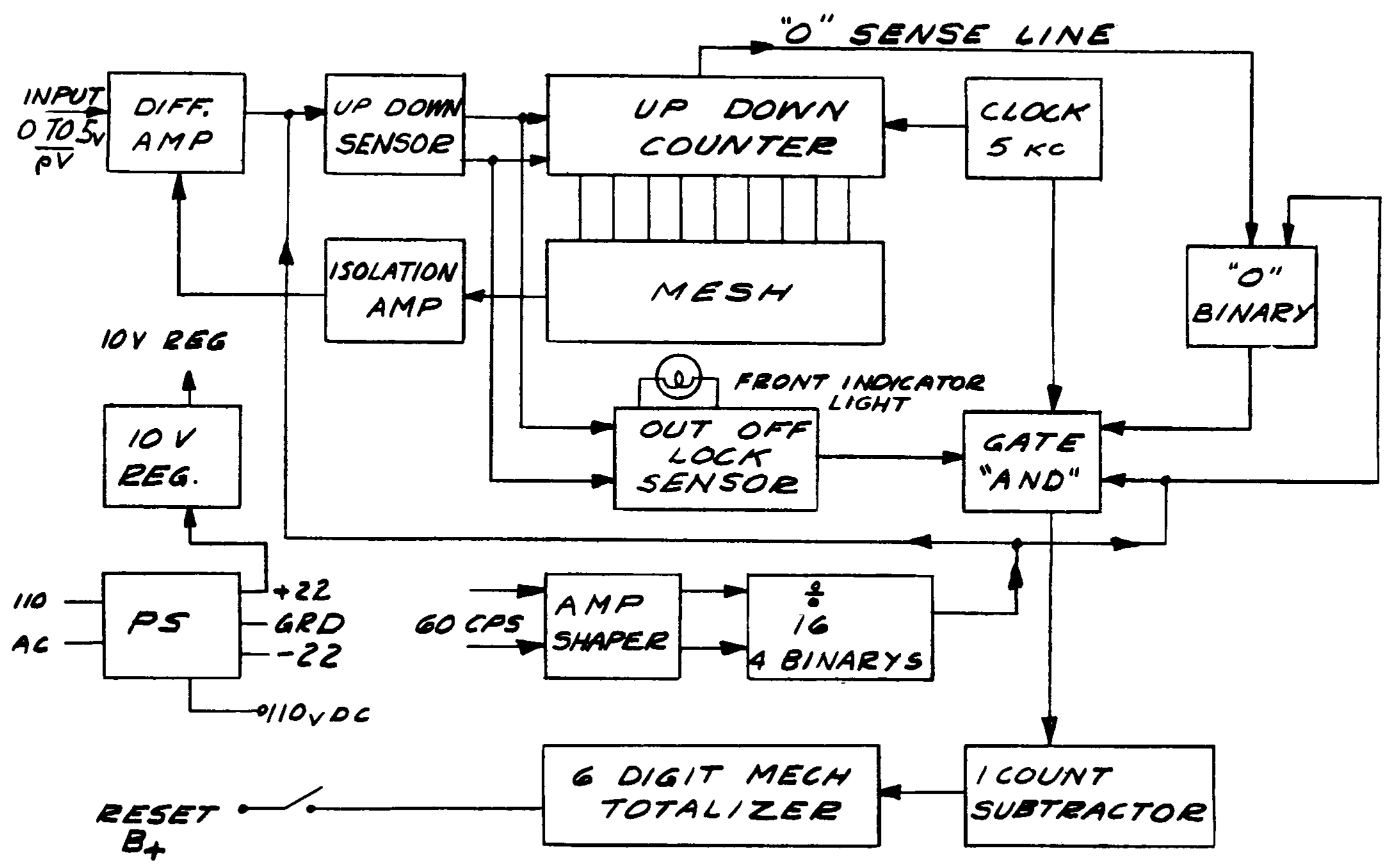

A9-41198-1

PERFORMANCE TESTS OF SYSTEM

A. Static Tests

In order to assess the accuracy of the required system measurements,

1) Fluid flow drag force
2) Fluid density
3) Fluid mass flow rate

a series of check-out tests are performed on the flowmeter components and system. Typical of these tests are:

1) Current through magnets needed to balance calibrated weights set on flow screen. These tests are conducted by observing the electronic readout signal $E_{out} = KV\sqrt{\rho}$ for known weights (accurate to 0.1%). Since at a force null the magnet current I^2 is proportional to the force F applied to the magnetic slug (to balance the applied screen load), and F in turn is proportional to ρV^2, a plot of $E_{out} = KV\sqrt{\rho}$ vs $\sqrt{\text{loading weight}}$ or I vs $\sqrt{F}$ should be a straight repeatable line. The repeatability of this line is indicative of the null repeatability of the force sensor, the hysteresis of mechanical and magnetic components, and sensitivity of the force servo. These tests are conducted at pressures and temperatures at the flow sensor expected during actual operation.

2) Output of density servo, $E_{out} = K\rho$, per various calibrated input capacitance. Here the density sensor is replaced by a calibrated three-terminal variable capacitor. The output of the density servo is then recorded for simulated operational capacitance values. Since the active and stray capacitance of the density sensor is known by actual measurement, the simulated capacitance values can readily be used to check the operational performance of the electronic readout of the fluid density.

3) Output of rate servo, $E_{out} = \overline{\rho V}$, for calibrated loading of the force screen and calibrated simulation of density sensor capacitance. Since this servo combines the $E_{out} = K_1 V\sqrt{\rho}$ and $E_{out} = K_2\rho$ to form $E_{out} = K_3\rho V$, checks of this combining are made by varying the load on the force screen and simulated density sensor capacitance. If a plot is now made of $E_{out} = K_3\overline{\rho V}$ vs $\sqrt{\text{loading weight}}$ for constant values of the density simulating capacitor, (d.s.c.), the points obtained should lie on a straight line. One straight line should be obtained for each d.s.c. setting, when the loading wt. goes from zero to full scale. In addition the change in $E_{out} = K_3\overline{\rho V}$, with a constant loading weight, for a percentage span of maximum density

(e.g. 55% to 95% max.) should correspond as nearly as possible with the percentage change in $E_{out} = (K_3 V\sqrt{\rho})(\sqrt{\rho})$. That is, if the density changes from 100% to 50%, since the force servo has a $\sqrt{\rho}$ factor, the change in $E_{out} = K_3\overline{\rho V}$ contributed by the density servo should only correspond to the change in $\sqrt{\rho}$ or E_{out} goes from 100% to 70.7% when the density simulating capacitor changes from 100% to 50% of its span. Now also since the $\sqrt{\rho}$ is approximated by a best fit straight line between 100% ρ max. and 50% ρ max., a change of the d.s.c. to simulate a 100% ρ max. to 75% ρ max. should change $E_{out} \square K_3\overline{\rho V}$ only one-half as much as a 100% ρ max. to 50% ρ max. d.s.c. change (Figure 13).

Date of Test: 2-8-65
By: T. A. Loftus, P. Bauer

SYSTEM STATIC CHECKS, WARM (300°K)

Applied Weight (Ounces)	Force Check		Multiplier Check	
	$E_{out} = K V\sqrt{\rho}$	Applied Weight	$E_{out} = \rho V$ (35 pf)*	$E_{out} = \rho V$ (38 pf)*
32	2.680	5.656	3.434	4.315
16	1.890	4.000	2.429	3.053
8	1.334	2.828	1.717	2.152
4	.944	2.000	1.217	1.520
2	.672	1.414	.868	1.079
1	.476	1.000	.616	.761
0.5	.338	.707	.439	.538

*Density simulating capacitance

NULL AND FORCE REPEATABILITY CHECKS

Applied Weight (Ounces)	$E_{out} = K V\sqrt{\rho}$ First Trial	Second Trial
40	2.997 ↓	2.997 ↑
32	2.680	2.680
16	1.890	1.890
8	1.334	1.335
4	.944	.944
2	.672	.672
1	.476	.476
0.5	.339	.337

FORCE REPEATABILITY CHECK

Cold tests in LN_2 - Force applied by calibrated current applied to opposing magnets. Record applied current equivalent voltage on opposite magnets necessary to give same value on $E_{out} \square K V \sqrt{\rho}$.

$E_{out} \square K V \sqrt{\rho}$	$E_{opposing\ magnet}$ First Trial	Second Trial	Third Trial	Fourth Trial
2.680	3.220 ↑	↓	3.226 ↓	3.233 ↑
1.890	2.274	2.268	2.266	2.278
1.334	1.608	1.591	1.597	1.600
.994	1.133	1.122	1.124	1.128
.672	.805	.788	.789	.798
.476	.576	.538	.548	.561
.339	.405	.362	.385	

FORCE REPEATABILITY CHECK

$E_{out} = K V \sqrt{\rho}$	$E_{opposing\ magnets}$ ↓	(Voltage drop across 50 ohm resistor) ↑	random	Order of Appli.		Order of Appli.				
2.500	3.074	3.073	3.073	⑥	3.070	⑩			3.073	[illegible]
1.890	2.319	2.321	2.321	④						
1.334	1.634	1.634	1.634	②						
.944	1.154	1.153	1.147	⑦	1.152	⑨	1.147	⑪	1.14[illegible]	
.672	.815	.818	.814	③						
.476	.572	.577	.569	⑤						
.339	.400		.397	①	.396	⑧				

FORCE REPEATABILITY CHECK

Nulled with wire hook on screen, forward, vertical.

Weight on Screen Ozs.	$E_{out} = KV\sqrt{\rho}$ First Trial	Second Trial	Third Trial	Fourth Trial	Fifth Trial	Sixth Trial	Seventh Trial	Eighth Trial
40	2.995↓	2.993↑						
32	2.678	2.677						
16	1.885	1.882						
8	1.324	1.327						
4	.935	.935						
2	.658	.659						
1	.456	.456						
.5	.315		.314					

$E_{out} = KV\sqrt{\rho}$	*$E_{opposing\ magnets}$ (Voltage drop across 50 ohm resistor)							
2.500	3.062↓	3.067↑		3.068.			3.071↓	
1.890	2.317	2.320		2.323	2.326↓			
1.334	1.640	1.644		1.643	1.643			
.944	1.164	1.160		1.163	1.178	1.165↑	1.175	1.168↑
.672	.832	.831		.835	.835			
.476	.588	.589		.596↑	.602			
.339	.418		.430↓		.444		.445	

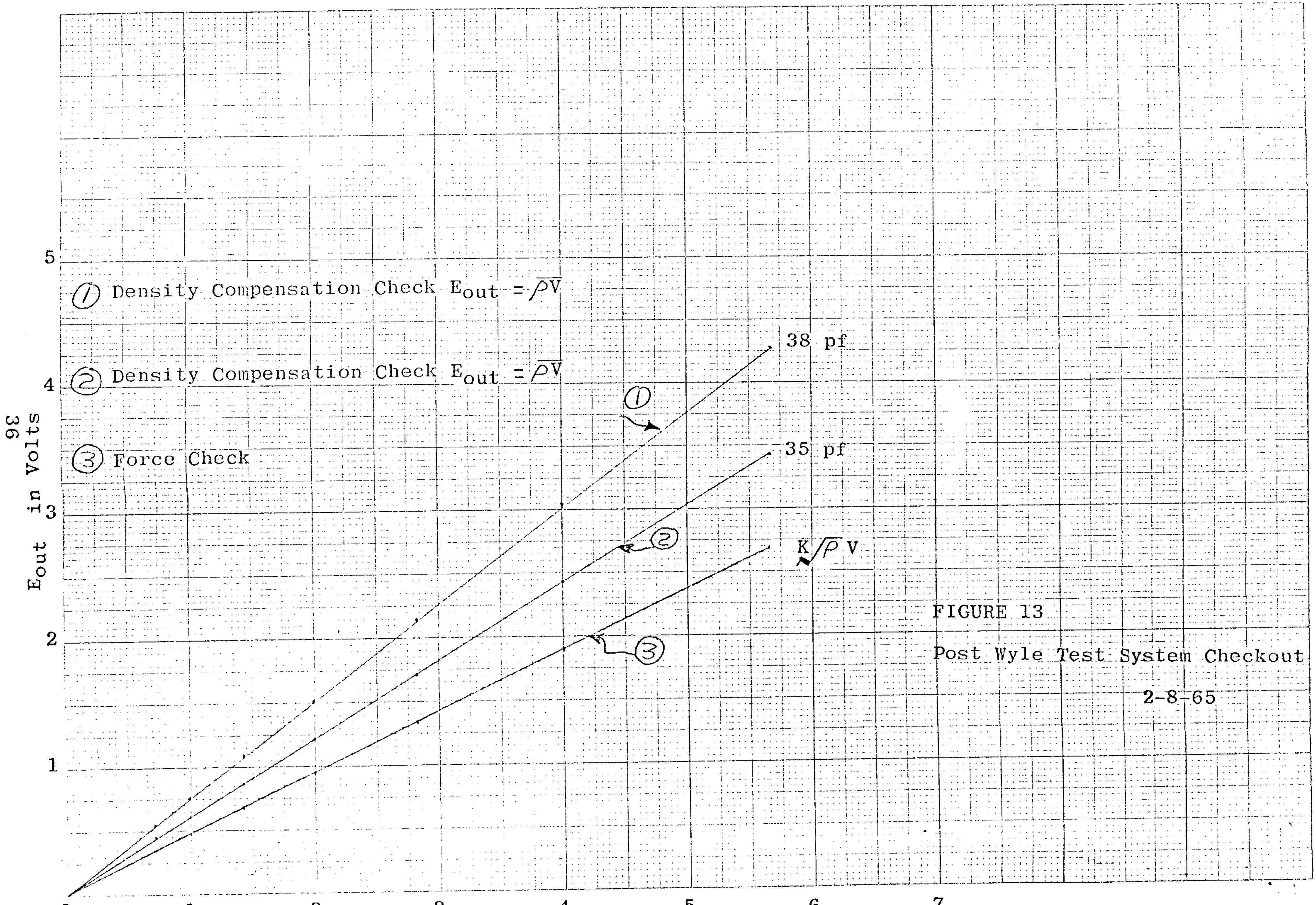

FIGURE 13

Post Wyle Test System Checkout

2-8-65

B. Dynamic Tests

Again to assess the accuracy of the required system measurements,

1) Fluid flow drag force
2) Fluid density
3) Fluid mass flow rate

the third measurement in particular, actual fluid flow tests must be made. While tests of the 1 and 3 measurement accuracies can be made in any fluid of known density, the information obtained must still be correlated with actual performance in LH_2. The main effect to be studied is performance of the flow sensor at the extremely low temperature (20^oK) encountered with LH_2 flow. Thus, three LH_2 flow tests have been conducted to date on the LH_2 mass flow meter.

In order to function accurately, the force sensor must be nulled against zero flow force, and this null cannot shift (mechanically or electrically) so as to cause a readout error of more than 0.5% of full scale indicated mass rate of flow. The other 0.5% of full scale mass rate of flow error is reserved for non-repeatability of the system due to insensitiveness to flow changes (lack of resolution). While a preliminary indication of these shifts can be obtained by static testing as previously outlined, the effect of dynamic forces on the flow and density sensors can only be assessed by flow tests preferably under actual LH_2 conditions.

Preliminary flow testing at Huntsville with LN_2 and LH_2 was encouraging and the only problems seemed to be the long cooling time required and some nulling difficulty with LH_2 due to the inability of the stand to hold a quiescent condition in the meter long enough to obtain a satisfactory null adjustment.

It was agreed that the unit was ready for calibration test and that the Wyle equipment would be capable of providing proper nulling conditions.

The first test at Wyle was stopped due to large quantities of foreign material in their system that disabled the honeycomb density sensors. It was also determined that a null instability problem existed which required further study test prior to rerunning the calibration test.

The density sections were rebuilt to repair the damage, a vacuum test tank made, and static tests with LH in the meter started.

This confirmed the existence of a null instability problem and the vacuum cover on the meter was removed for the first time to find its cause.

Both of the outer support diaphragms (flat when initially assembled) were buckled in the region of the three intermediate outer tie points. This was caused by large temperature differential on cooling between the inside of the support (clamped to the housing) and the outside clamped at six points to the outer sensitive (moving) frame. Tension in the support during cool down was sufficient to allow it to pull out at the three intermediate points. These points on each of the supports are clamped with one screw. The other three points opposite the housing lever bosses are clamped with two screws, and being quite close to the three large housing bosses probably do not see as much temperature differential. Slipping at the three intermediate points would also allow the outer frame to distort and relieve stress at the other points.

Everything else seemed to be correct and it was agreed that no additional slipping would occur in that it had provided itself with the necessary slack; there being insufficient stiffness in the support for it to push itself back. Further study and static testing at running temperature indicated that a special testing technique might be set up for preventing the null shifts caused by the buckled supports. LH_2 testing was then started with temporary servo modification that would permit applying external power to the unused (opposite) set of magnets. The meter cover was replaced but not sealed to also see if this would be a satisfactory method for testing. This to allow ease of subsequent access to the outer mechanism if required.

We were able to prevent null shifts at LH_2 temperature by not allowing reverse flow forces on the meter during forward operation and vice versa.

This we felt could be accomplished during the calibration test by applying sufficient external power to the reverse flow magnets between runs while the calibration tank was being refilled and a decision was made to test in this manner rather than to modify the meter. An additional static test with LH_2 was made to reaffirm this method and the use of an unsealed cover.

Initial tests at Wyle showed that this method of preventing null shift was not satisfactory under dynamic conditions and a decision was made to modify the meter by removing the three intermediate points in each of the supports by cutting a section out of each.

Null characteristics during cool down prior to testing following the modification were even better than expected. No sudden changes occurred as previously noted. The null shifted gradually during cool down and when stabilized would repeat following forward flows and reverse flows (prior to test) without external power to the opposite magnets.

At start of the test for the first few runs the null was steady then shifting started and became progressively worse. Readjustment also became more and more difficult and at the end of the test it suddenly became impossible to find the null.

It was later learned that the vacuum pump was not on the chamber during the test, (it was on for all previous testing) that twice during the test it was put on the chamber to restore its vacuum.

Both times it was noted that the line and meter between runs warmed so as not to hold liquid at all between runs and pumping at the end of the test restored what seemed to be normal meter operation.

It is our contention that frost accumulation on the outer sensitive parts and abnormal temperature variation (all caused by the vacuum condition) prevented a representative test.

Meter function observed during cool down, on runs prior to, and for the first few test runs indicated that the modification removed or satisfactorily reduced the null stability problem and that the data recorded would have been much better.

The loss of vacuum prevented quiescent condition between runs for accurate null observation, subsequent static test and examination support the above.

The following graphs give the data reduced from the recorded outputs of the Bendix Electronic Readout during the two periods of Wyle tests.

Also included for cross reference purposes are the Wyle outputs.

A plot of the Bendix rate of flow output against the Wyle rate of flow (Figure 15) should give a straight line. If the Bendix rate is plotted vertically and the Wyle rate horizontally, the horizontal spread of the Bendix rate should fall within a $\pm$ 1% band (of Wyle 15 lb/sec. full scale). When the extremes of this band are connected, they form two parallel lines with the straight line of the data.

Generally, the data falls equally on either side of a best straight line fit. But, if the data falls more nearly on two parallel lines, an explanation is needed. Two parallel lines correlating a group of data points arise from a constant force being added to the force servo. Because flow existing during a force null during supposedly quiescent conditions is never exactly repeatable, the data from such error would not form a second parallel line. In fact, a consideration of the resultant change in magnet gap shows that such an error force at null will tilt the normal zero null error data line with respect to the normal zero null error line. But if no null error is present, and a constant force is added to the flow force during flow measurement, the result is a set of two parallel lines; one for zero constant added force and a second for unit constant added force.

In a flow sensor of the present type, such a constant added force could be obtained from oil-can behavior of pivot and support diaphragms. These diaphragms in oil-can behavior have two non-stable equilibrium points, either of which could contribute a constant added error force during flow.

When the Bendix totalizer data is considered, an empirical way is available to trace the flow errors back to the force sensor. Considering that the rate should contribute a totalizer error proportioned to its deviation from a straight line, we reduce the actual Bendix rate data force run in proportion to the totalizer excess over a given fixed count. Choosing 81.000 as the proper totalizer constant for a constant total mass of fluid measured, say that 82.000 is the count obtained with an indicated rate of 52.0% of full scale. The corrected rate then is:

$$\frac{81.000}{82.000}\ 52.0 = 51.3$$

A plot of the corrected Bendix rate against the actual Wyle rate (Figure 16) should be a straight line. If this is not true, then the points which lie off this straight line indicate a totalizer contribution to the total counts. Thus if no totalizer error is present very little data scatter should occur about this straight line.

Carrying the procedure a step further, the Bendix $\sqrt{\text{force}}$ or $E_{out} = KV\sqrt{\rho}$ data (Figure 17) may be corrected by the percentage deviation of the rate data from a straight line. Thus if the electronics is not properly combining the $E_{out} = K\rho$ and $E_{out} = KV\sqrt{\rho}$ signals, the rate error will not be in proportion to the $E_{out} = KV\sqrt{\rho}$ error. Since the runs on 1/29/65 were made at nearly constant density ($\pm$ 0.2% point), if the corrected $\sqrt{\text{force}}$ data lies on a straight line, the combining of the $\sqrt{\text{force}}$ and density signals was performed correctly, and the error has been traced to the force sensor (Figure 18).

FLOWMETER CALIBRATION DATA SHEET

CUSTOMER	MANUFACTURER	CALIBRATION DATE	CALIBRATION STANDARD
NASA	BENDIX	8/5/64	199.11 #
JOB NUMBER	MODEL NUMBER	TEST ENGINEER	CALIBRATION FLUID
44722-03		ROBINETT	LIQUID HYDROGEN
REPORT NUMBER	SERIAL NUMBER	ENGINEERING APPROVAL	BAROMETRIC PRESSURE
			14.25 PSIA

Run No.	Elapsed Time Min.	Elapsed Time Sec.	$\dot{W}$ p.p.s	Bendix Rate % 100	Bendix Force % 100	Totalizer Counts	Bendix Density % 100	Inlet Pressure (PSIA)	Temp. Ohms	Temp. °R
1	0.2718	16.308	12.209	———	———	———	Bad	51.75	170.05	38.90
2	0.2439	14.634	13.606	95.5	99.5	103378	Bad	50.25	170.07	39.01
3	0.2480	14.880	13.381	103.5	101.0	108598	Bad	51.25	170.0	38.62
4	0.2343	14.040	14.182	95.0	97.5	97857	13.1	50.25	170.0	38.62
5	0.2368	14.208	14.014	102.5	97.5	105908	Bad	48.85	169.93	38.21
6	0.2330	13.980	14.242	101.0	98.5	103846	Bad	50.25	169.93	38.21
7	0.2279	13.668	14.528	102.0	100.5	102285	Bad	49.45	169.82	37.58
8	0.2259	13.554	14.690	92.0	99.5	Bad	Bad	48.95	169.82	37.58
9	0.2277	13.662	14.514	———	102.5	Bad	Bad	49.25	169.83	37.64
10	0.2262	13.572	14.671		101.5	Bad	1.2	50.25	169.87	37.87
11	0.2342	14.052	14.170	102.0	98.75	105975	2.9	49.65	169.87	37.87
12	0.3004	18.024	11.047	73.5	72.0	77098	Bad	52.45	169.88	37.93
13	0.3205	19.230	10.354	63.25	65.0	89248	11.75	54.75	169.86	37.81
14	0.3502	21.012	9.476	56.25	58.0	86.728	12.6	51.25	169.86	37.81
15	0.3862	23.172	8.593	49.5	51.5	85.023	12.4	51.25	169.85	37.76
16	0.4567	27.402	7.266	41.75	43.5	84624	12.5	50.25	169.84	37.70
17	0.5419	32.514	6.124	36.5	38.5	87220	12.8	51.05	169.85	37.76
18	0.6103	36.618	5.438	32.5	34.5	87694	13.0	51.55	169.85	37.76
19	0.6900	41.400	4.809	28.5	29.5	86346	12.8	52.05	169.85	37.76
20	0.9353	56.118	3.548	22.5	23.5	93705	13.0	49.75	169.86	37.81
21	1.2295	73.770	2.699	12.5	13.25	66935	13.0	49.75	169.85	37.76
22	2.5288	151.728	1.312	16.5	17.0	———	13.0	49.25	169.88	37.93
23	2.5278	151.668	1.313	9.0	9.5	———	13.0	48.25	169.88	37.93
24	0.2744	16.464	12.094	81.5	79.5	98587	Bad	49.75	169.92	38.16
25	0.4433	26.2598	7.485	44.5	46.5	87379	13.5	50.25	169.92	38.16
26	1.3034	78.204	2.546	18.0	18.5	101954	13.5	50.25	169.90	38.04
27	0.4579	27.474	7.247	45.0	47.5	89243	13.0	50.25	169.82	37.58
28	0.4649	27.894	7.138	45.25	47.5	90344	Bad	50.75	169.90	38.04
29										
30										

REMARKS:

FLOWMETER CALIBRATION DATA SHEET

CUSTOMER	MANUFACTURER	CALIBRATION DATE	CALIBRATION STAN
NASA	BENDIX	8/4/64	199.11#
JOB NUMBER	MODEL NUMBER	TEST ENGINEER	CALIBRATION FLUI
44722-3		ROBINETT	LIQUID HYDROGEN
REPORT NUMBER	SERIAL NUMBER	ENGINEERING APPROVAL	BAROMETRIC PRESS
			14.31 PSIA

Run No.	Elapsed Time Min.	Time Sec.	$\dot{W}$ LB/Sec	Bendix Rate % 100	Bendix Force % 100	Bendix Density % 100	Total Count Totalizer	Inlet Press. (PSIA)	Temp. Ohms	Temp. °R	ΔP
1	1.1308	67.848	2.935	19.6	25.0	46.0	58364	46.3	169.90	38.04	0
2	0.9505	57.030	3.491	23.0	30.0	46.8	64921	43.8	169.87	37.87	0
3	0.6566	39.396	5.054	22.0	29.5	47.0	41726	49.3	169.92	38.16	0.1
4	0.5368	32.208	6.182	30.5	48.5	47.0	54411	48.3	169.90	38.04	0.2
5	0.5554	33.324	5.975	Bad	43.5	Bad		47.8	169.95	38.32	0.2
6	0.5966	35.436	5.619	101.0	39.5	Bad		48.3	169.90	38.04	0.1
7	0.6830	40.980	4.859	86.0	33.5	Bad		47.8	169.95	38.32	0.08
8	2.0465	122.790	1.622	10.0	12.0	46.0	14173	46.8	170.02	38.73	0
9	0.4991	29.946	6.649	34.0	43.0	46.0	73000	47.0	169.98	38.50	0.30
10	0.4535	27.210	7.318	Bad	Bad	Bad		47.4	170.00	38.62	0.4
11	0.4491	26.946	7.389	36.5	46.5	45.5	72097	47.6	120.00	38.62	0.4
12	0.3059	18.354	10.848	Bad	63.0	Bad		48.3	169.95	38.32	0.9
13	0.3143	18.858	10.558	51.5	66.0	Bad	74763	47.3	169.95	38.32	0.8
14	0.3045	18.270	10.898	52.5	67.0	46.0	68692	48.9	169.93	38.21	0.82
15	0.3128	18.768	10.609	Bad	Bad	Bad		47.3	169.95	38.32	0.85
16	0.3064	18.384	10.831	54.0	69.0	46.0	72332	48.8	169.75	38.32	0.84
17	0.2200	13.200	15.084	79.0	101.5	46.0	76965	47.6	169.95	38.32	1.80
18	0.2181	18.086	15.215	Bad	101.5	Bad		48.1	169.95	38.32	1.60
19	0.2200	13.200	15.084	Bad	101.5	Bad	77273	47.7	169.95	38.32	1.60
20	0.2244	13.464	14.788	77.5	99.5	Bad	76363	47.3	169.97	38.44	1.60
21	0.2220	13.320	14.948	Bad	101.0	Bad		46.8	169.95	38.32	1.60
22											
23											
24											
25											
26											
27											
28											
29											
30											

REMARKS:

TEST DATE: 1/29/65 CUSTOMER: NASA DATA SHEET BENDIX MASS FLOWMETER DATA RED'D

TEST TIME: ΔW = 199.11 lbs JOB NO.: 44722-03 BY: F. E. Robinett

Run No.	Time Min.	Time Sec.	Inlet Temp. (ohms)	Inlet Temp. (°R)	Inlet Press. (PSIA)	ΔP In.Hg.	Rate #/Sec.	Bendix Rate % 84	Bendix Force % 100	Bendix Density 100-1100	Bendix Totalizer	81.000+ Bendix Total	Corrected Bendix Rate	Corrected Bendix Force	Bendix Totalizer ÷ Time(M)	Wyle Spec Weight FT³/LB
1	—	—	170.25	40.05	35.3	0	—	—	20.12	71.2	—	—	—	—	—	—
2	.5219	31.314	170.27	40.16	39.3	0	6.3555	36.1	20.14	71.1	83627	.96859	34.77	20.07	160,236	—
3	.5160	30.960	170.30	40.34	38.3	0	6.431	37.1	21.23	71.3	84851	.95461	35.42	20.27	164,440	—
4	.5065	30.390	170.41	40.97	40.0	—	6.552	37.5	21.62	71.3	83158	.96477	36.18	20.86	165,761	—
5	.5159	30.954	170.20	39.76	39.5	—	6.432	38.6	22.02	71.3	87791	.92265	35.61	20.32	170,171	—
6	.5178	31.068	170.23	39.93	39.7	—	6.409	37.2	21.44	71.2	85204	.75066	35.36	20.39	164,550	—
7	.8316	49.896	170.30	40.34	43.3	—	3.991	26.5	15.5	71.1	98767	.84011 Recall	21.73	12.71	118,767	—
8	.8708	52.248	170.31	—	41.30	—	3.810	25.2	14.8	71.2	98571	.82174	20.71	12.16	113,196	—
9	.4062	24.372	170.15	—	45.50	—	8.170	45.1	26.2	71.0	81280	.97656	44.74	26.11	200,095	—
10	—	—	170.22	—	43.2	—	—	—	24.6	70.5	81813	.98734	—	24.34		—
11	.4390	26.340	170.20	39.76	43.3	—	7.559	41.5	24.3	70.5	81574	.97296	41.21	24.13	185,815	—
12	.3697	22.182	170.30	—	43.3	—	8.976	49.0	28.6	70.6	80719	1.00348	47.12	28.70	218,336	—
13	.3095	18.570	170.30	—	47.5	—	10.722	—	—	70.6	(76471)	Interrupted Count			—	—
14	—	—	—	—	—	—	—	—	—	—	—	—	—	—	—	—
			15 PT. CALIBRATION START													
1	.2995	17.970	170.24	39.99	48.3	1.7	11.080	61.9	73.7	70.5	81.729	.98866	61.20	72.56	273,553	.2332
2	.3039	18.234	170.27	40.16	48.3	1.65	10.919	59.5	70.8	70.7	80.469	1.00660	57.89	71.27	264,788	.2333
3	.3594	21.564	170.20	39.76	44.3	1.25	9.233	50.0	58.5	70.6	79.413	1.01896	50.75	57.61	221,183	.2328
4	.3985	23.910	170.24	39.99	41.3	1.10	8.327	46.4	53.8	70.5	71.930	.78865	45.77	53.19	205,576	.2334
5	.4149	24.849	170.22	39.98	44.8	1.05	7.998	43.8	50.4	70.5	81.541	1.00570	44.05	50.69	174,121	.2330
6	.6081	36.486	170.22	39.88	39.8	.75	5.457	33.7	33.6	70.4	91.660	.85351	27.95	33.57	150,465	.2333
7	.5799	34.794	170.17	39.59	41.3	.80	5.722	35.4	40.0	70.5	91.210	.88506 Adjusting Null	31.44	35.52	157,286	.2325
8	.7400	44.400	170.28	40.22	39.7	.70	4.484	29.8	33.1	70.4	79.479	.82250 Adjusting Null	24.51	27.22	133,080	.2339
9	.7200	43.200	170.22	39.88	40.2	.75	4.609	27.5	32.3	70.5	94.414	.85792 Adjusting Null	25.31	27.71	131,131	.2332
10	.9329	55.974	170.22	39.88	39.7	.65	3.557	23.6	25.1	70.5	97.222	.81635	19.27	20.49	106,351	.2332
11	.9558	57.348	170.22	39.88	40.6	.65	3.471	25.0	24.1	70.6	108.550	.74620	19.66	20.22	113,570	.2332
12	1.2220	73.320	170.20	39.76	39.3	.50	2.715	18.5	18.7	70.5	111.880	.79505	14.71	14.87	93,312	.2330
13	1.1687	70.122	170.20	39.76	37.7	.50	2.839	19.3	17.6	70.6	101.407	.77576	15.42	15.66	86,769	.2330
14	.2780	16.680	170.17	39.59	49.5	2.20	11.937	72.0	75.8	70.5	88.103	.92042	66.27	78.77	316,558	.2322
15	.2890	17.340	170.21	39.81	48.5	2.10	1.482	67.4	79.7	70.5	84.856	.75456	64.34	76.08	273,619	.2327
16	.4272	25.632	170.15	39.48	42.8	1.00	7.768	44.6	51.4	70.5	24.764	.75334	42.52	47.00	173,856	.2322
17	.3746	22.476	170.20	39.76	43.7	1.25	8.858	50.7	59.0	70.5	73.952	.76484	48.72	56.73	224,111	.2327

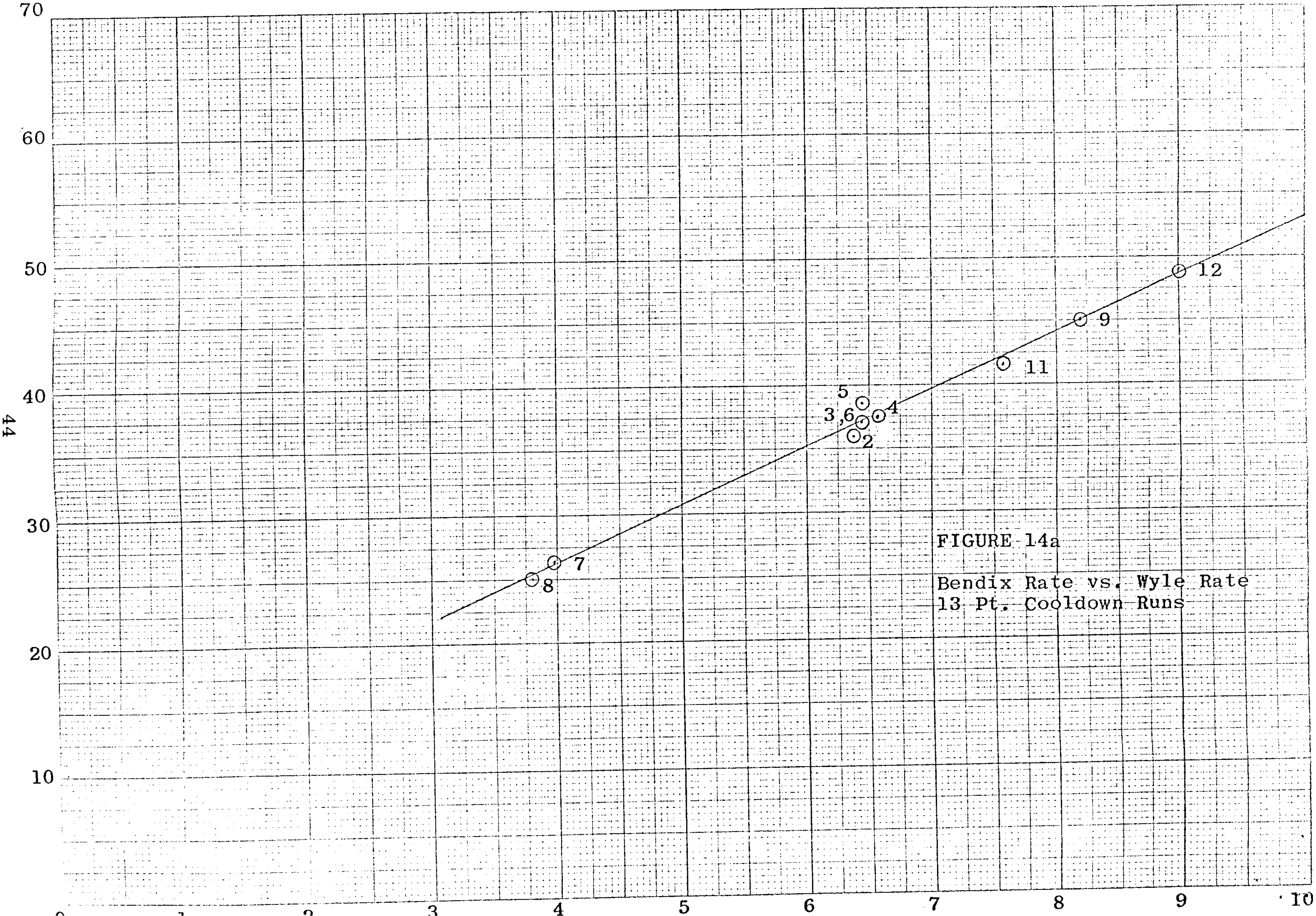

FIGURE 14a

Bendix Rate vs. Wyle Rate
13 Pt. Cooldown Runs

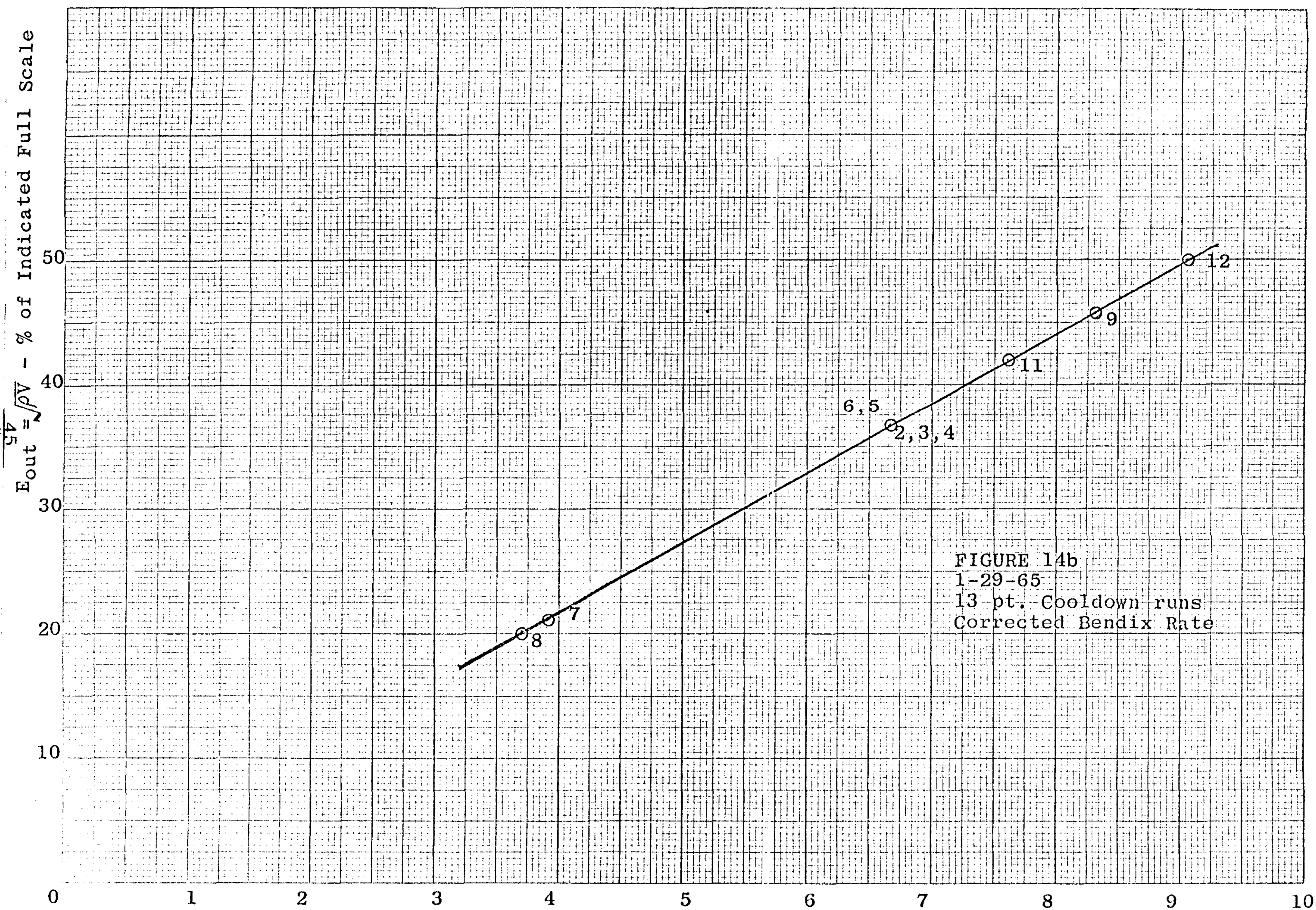

FIGURE 14b
1-29-65
13 pt. Cooldown runs
Corrected Bendix Rate

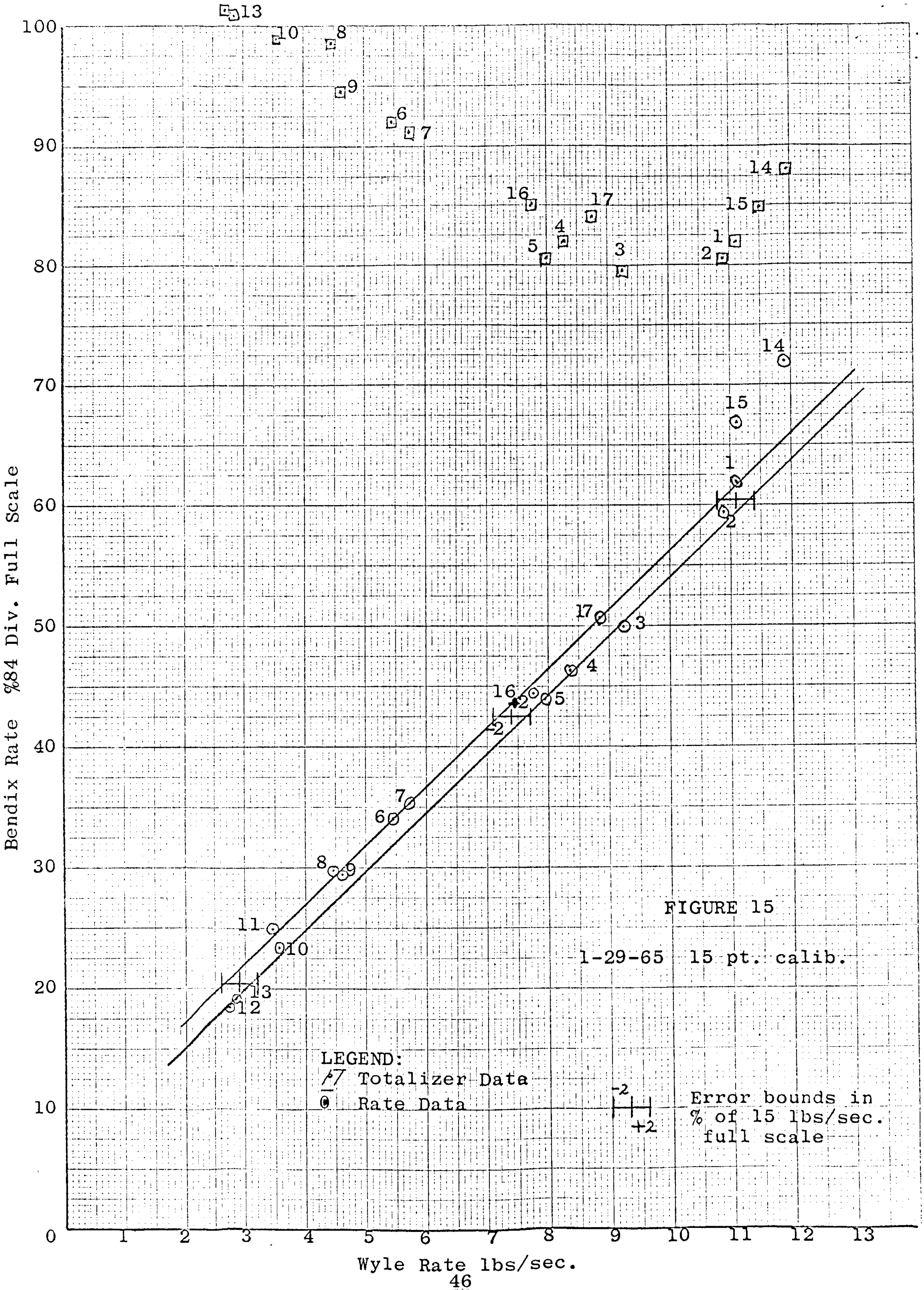

Bendix Rate %84 Div. Full Scale
Wyle Rate lbs/sec.
0
1
2
3
4
5
6
7
8
9
10
11
12
13
10
20
30
40
50
60
70
80
90
100
FIGURE 15
1-29-65 15 pt. calib.
LEGEND:
Totalizer Data
Rate Data
-2
+2
Error bounds in % of 15 lbs/sec. full scale

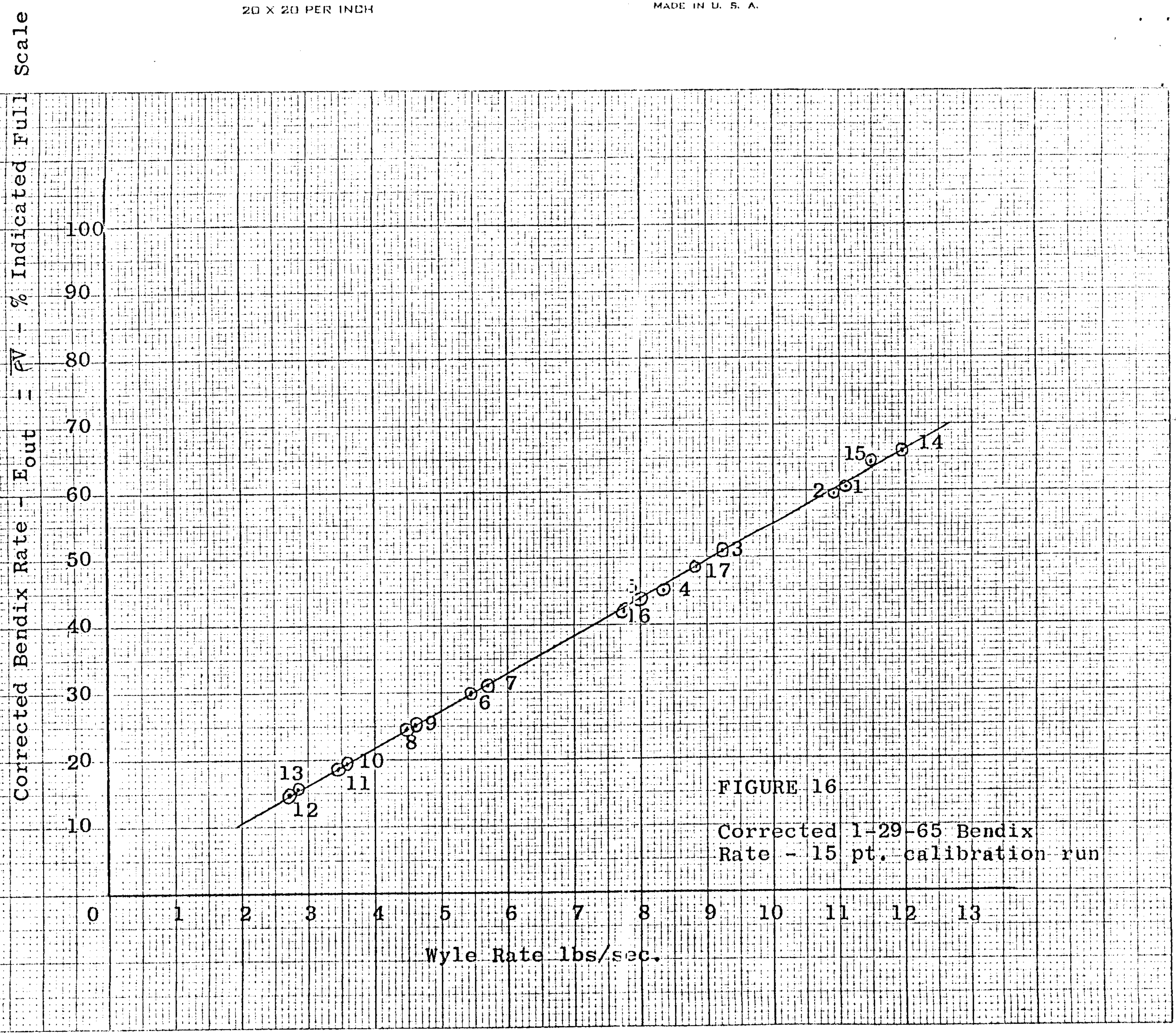

FIGURE 16

Corrected 1-29-65 Bendix Rate - 15 pt. calibration run

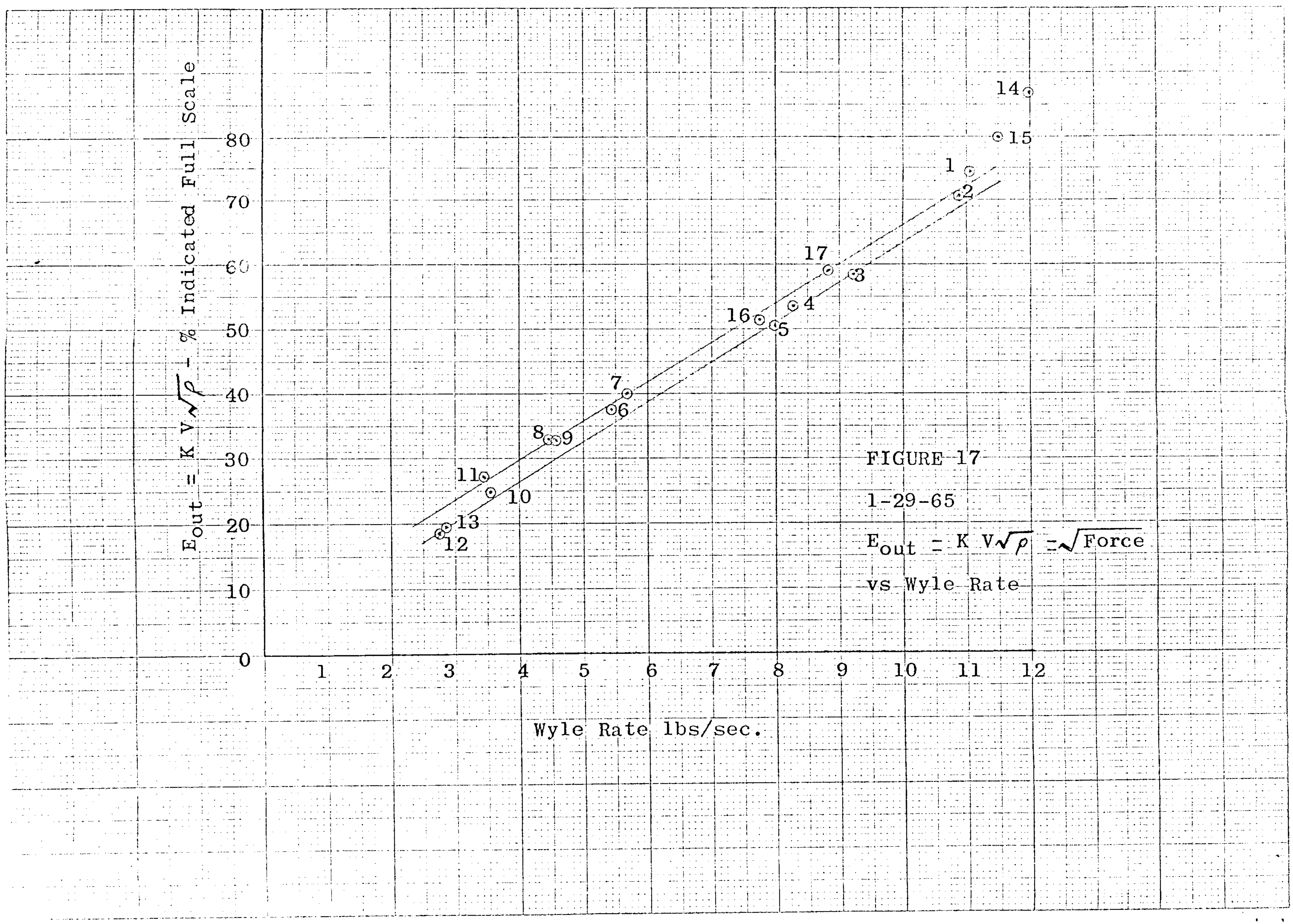

FIGURE 17

1-29-65

$E_{out} = K V\sqrt{\rho} = \sqrt{Force}$

vs Wyle Rate

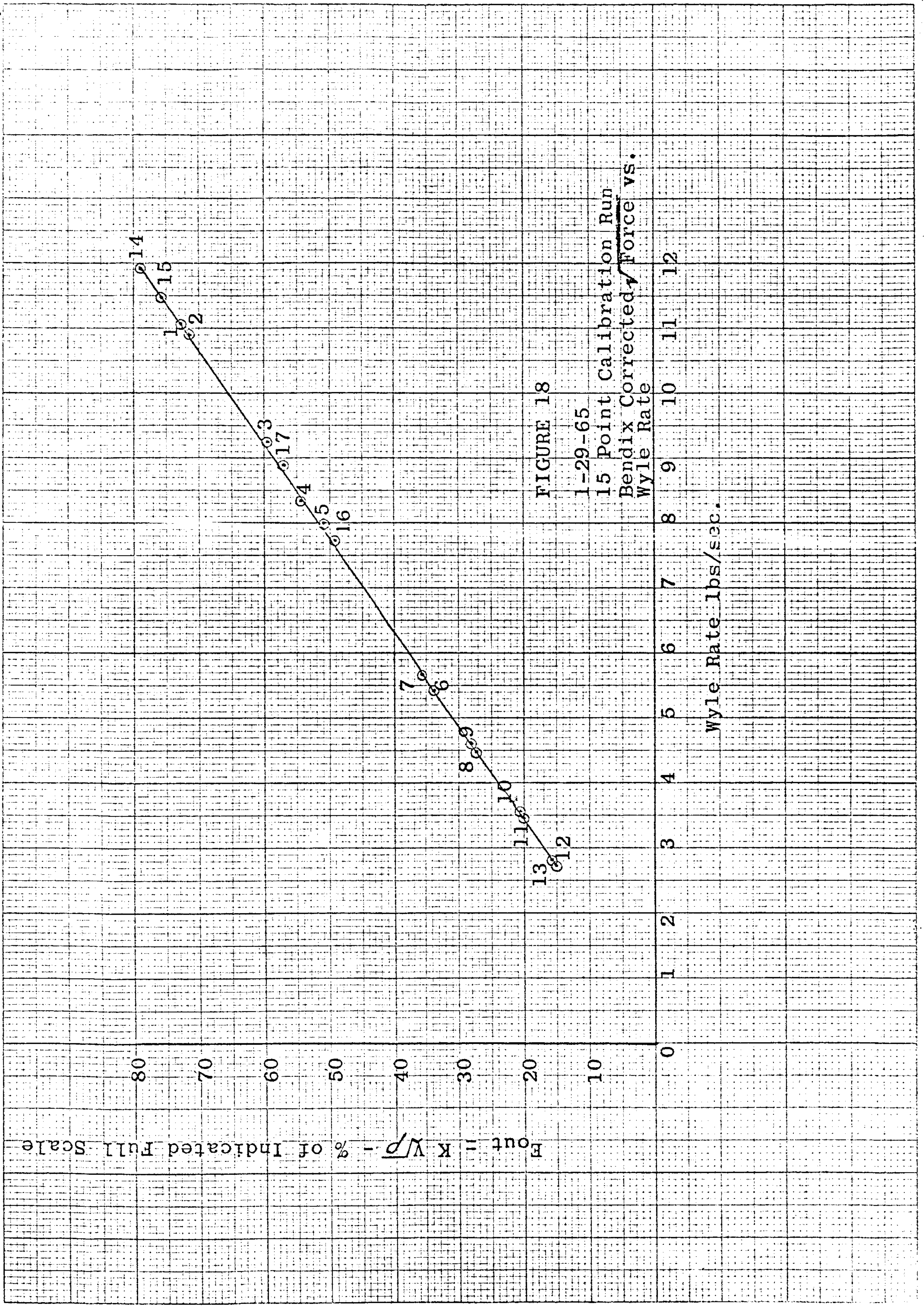

FIGURE 18

1-29-65

15 Point Calibration Run

Bendix Corrected √Force vs.

Wyle Rate

TEST DATE: 2/1/65   CUSTOMER: NASA   DATA SHEET   BENDIX MASS FLOWMETER   DATA RED'D

TEST TIME: ΔW = 199.11 #   JOB NO.: 44722-03   BY: F. E. Robinett

Run No.	Time Min.	Time Sec.	Inlet Temp. (ohms)	Inlet Temp. (°R)	Inlet Press. (PSIA)	ΔP (In.Hg)	Rate (#/Sec)	Bendix Rate % 84	Bendix Force %100	Bendix Density 100-%100	Bendix Totalizer	Corrected Bendix Rate	Corrected Bendix Force	Bendix Totalizer ÷ Time (#)	
1	1.7142	102.852	170.32	40.45	35.2	0.3	1.936	13.3	—	29.8	103.548	10.4	—	60.406	
2	1.6571	99.426	170.33	40.50	35.2	0.3	2.003	12.9	—	29.8	96.833	10.8	—	58.435	
3	1.3930	83.580	170.28	40.22	43.2	0.4	2.382	18.0	18.5	30.6	104.631	14.0	14.33	75.112	
4	0.7545	45.270	170.30	40.34	43.2	0.5	4.398	29.8	33.1	30.3	99.270	24.3	27.00	131.571	
5	0.5808	34.848	170.34	40.56	40.2	0.6	5.714	36.1	41.0	30.3	92.581	31.6	35.86	159.403	
6	0.4391	26.346	170.40	40.91	39.2	0.95	7.557	47.6	55.5	29.8	91.878	41.8	48.92	209.242	
7	0.4602	27.612	170.40	40.91	37.0	0.8	7.211	42.9	49.2	29.7	86.559	40.2	46.02	188.090	
8	0.4288	25.728	170.35	40.62	37.0	0.8	7.739	45.7	52.8	29.8	86.154	43.0	49.61	200.919	
9	0.3946	20.976	170.37	40.74	48.7	1.4	9.492	—	—	29.5	90.886	—	—	259.971	Lost Liquid at end of run
10	0.3464	20.784	170.40	40.91	47.7	1.2	9.580	59.6	69.4	29.7	88.857	54.3	63.23	256.516	
11	0.3128	18.768	170.36	40.68	48.3	—	10.609	66.1	78.2	29.7	90.027	59.5	70.38	287.810	
12	0.5890	35.340	170.37	40.74	39.4	—	5.634	35.5	39.9	30.5	91.996	31.3	35.13	156.190	
13	0.5844	35.064	170.35	40.62	40.8	—	5.678	37.8	42.6	30.8	105.462	29.0	32.71	180.462	
14	0.4699	28.194	170.38	40.79	49.2	—	7.062	42.4	48.5	30.6	87.712	39.2	44.79	186.661	
15	0.5036	30.216	170.40	40.91	46.5	—	6.589	41.9	48.3	30.7	93.305	36.4	41.93	185.276	
16	0.4996	29.976	170.33	40.50	45.2	—	6.642	41.8	52.5	31.0	90.222	37.6	47.15	180.588	
17	0.2881	17.286	170.39	40.85	48.2	—	11.518	67.5	79.8	30.0	84.761	64.5	76.22	294.207	
18	0.2827	16.962	170.35	40.62	48.0	—	11.739	65.6	77.5	30.3	80.828	65.7	77.69	285.914	
19	0.8999	53.994	170.30	40.34	42.9	—	3.688	25.4	27.2	30.5	102.043	20.2	21.60	113.394	
20															

Runs 11 thru 19 P Transducer not working

Temperature & Pressures ± 0.5%

Time ± 0.0002 Minutes

Average Rate 0.2%

Weight ± 7 grains

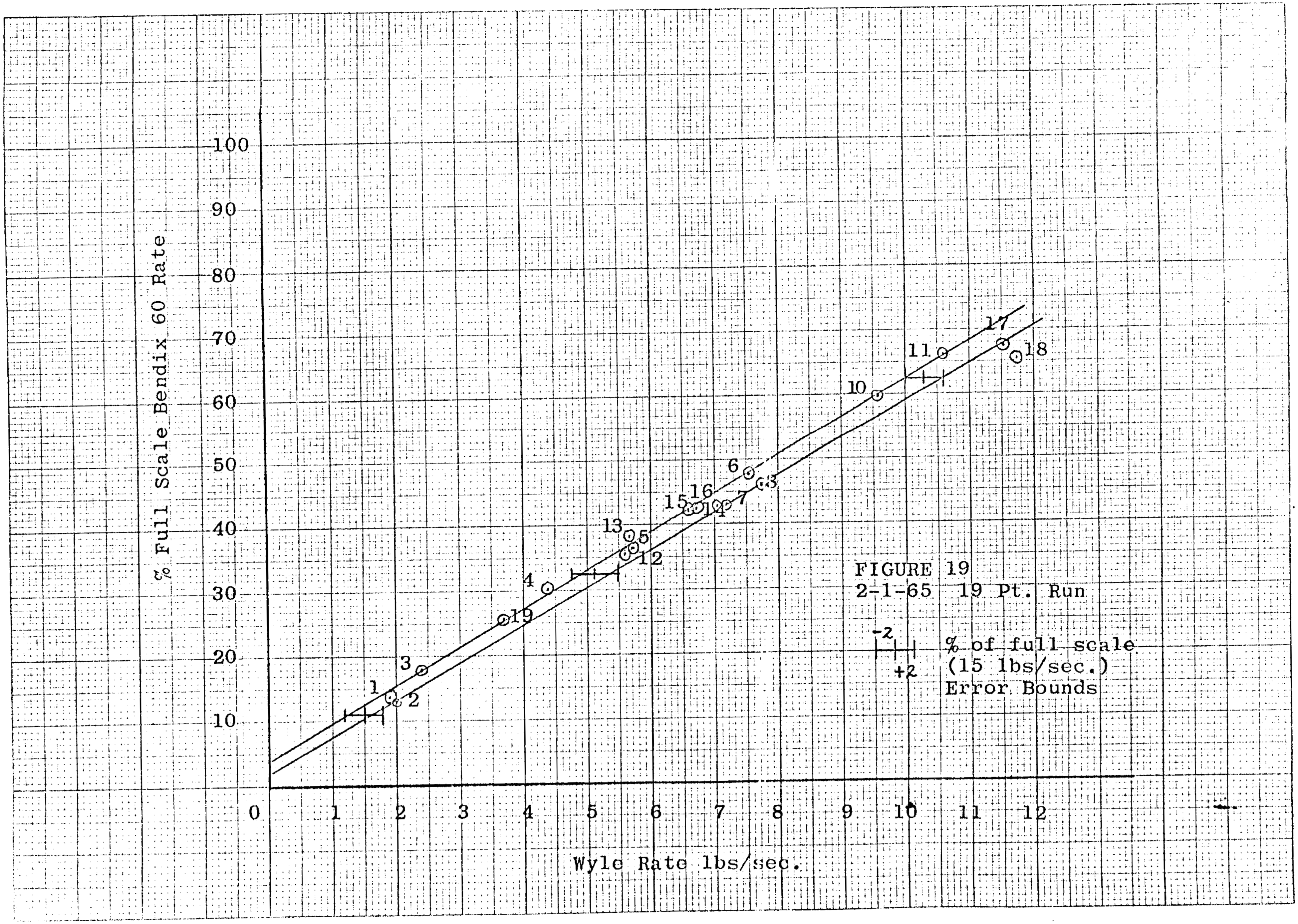

FIGURE 19
2-1-65 19 Pt. Run

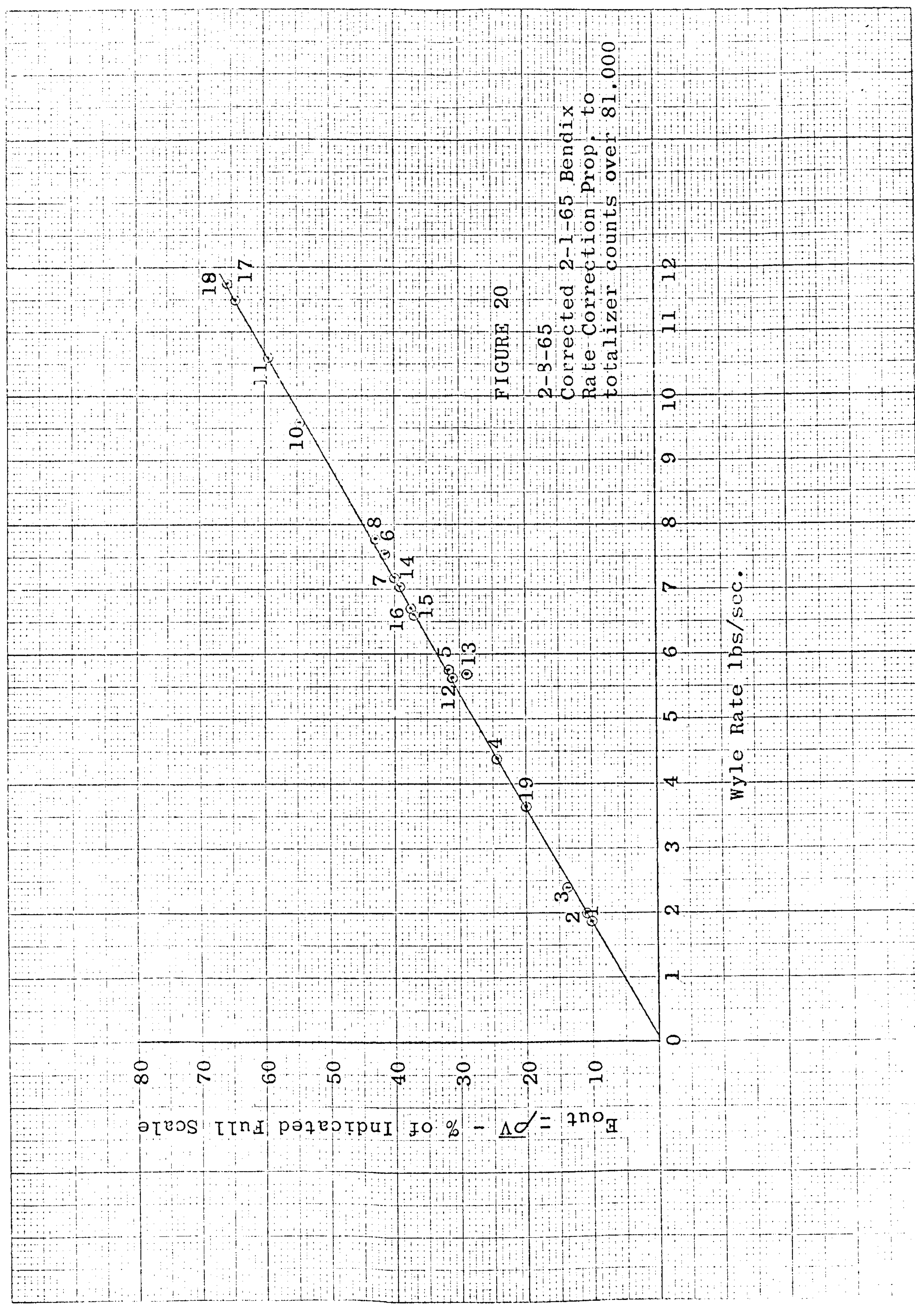
FIGURE 20
2-3-65
Corrected 2-1-65 Bendix
Rate Correction Prop. to
totalizer counts over 81.000
Wyle Rate lbs/sec.
E out = ΔV - % of Indicated Full Scale
0 1 2 3 4 5 6 7 8 9 10 11 12
10 20 30 40 50 60 70 80
NO. 340-20 DIETZGEN GRAPH PAPER
20 X 20 PER INCH
EUGENE DIETZGEN CO.
MADE IN U. S. A.

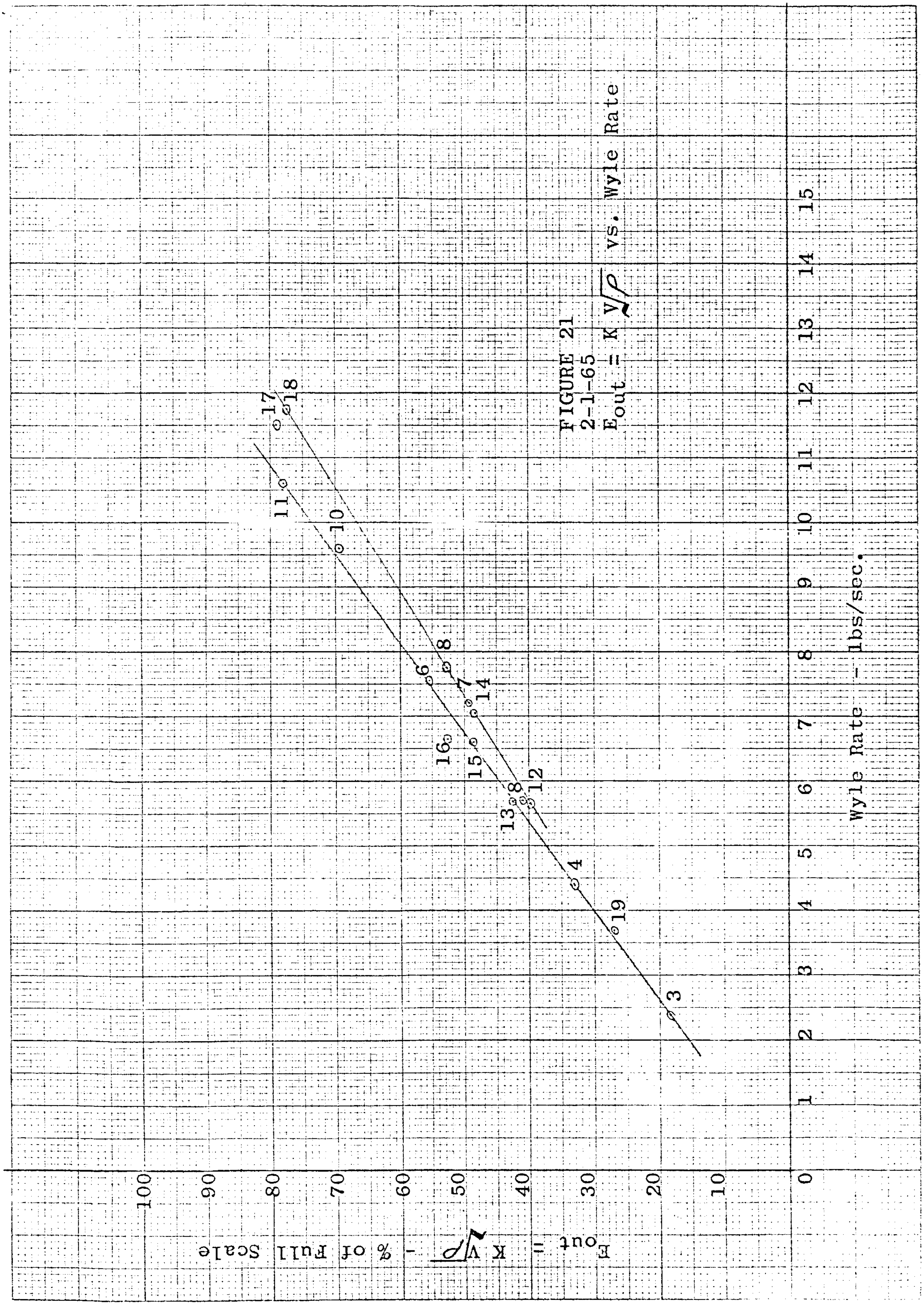
FIGURE 21
2-1-65
$E_{out} = K\, V\sqrt{\rho}$ vs. Wyle Rate
Wyle Rate - lbs/sec.
$E_{out} = K\, V\sqrt{\rho}$ - % of Full Scale
0
1
2
3
4
5
6
7
8
9
10
11
12
13
14
15
10
20
30
40
50
60
70
80
90
100

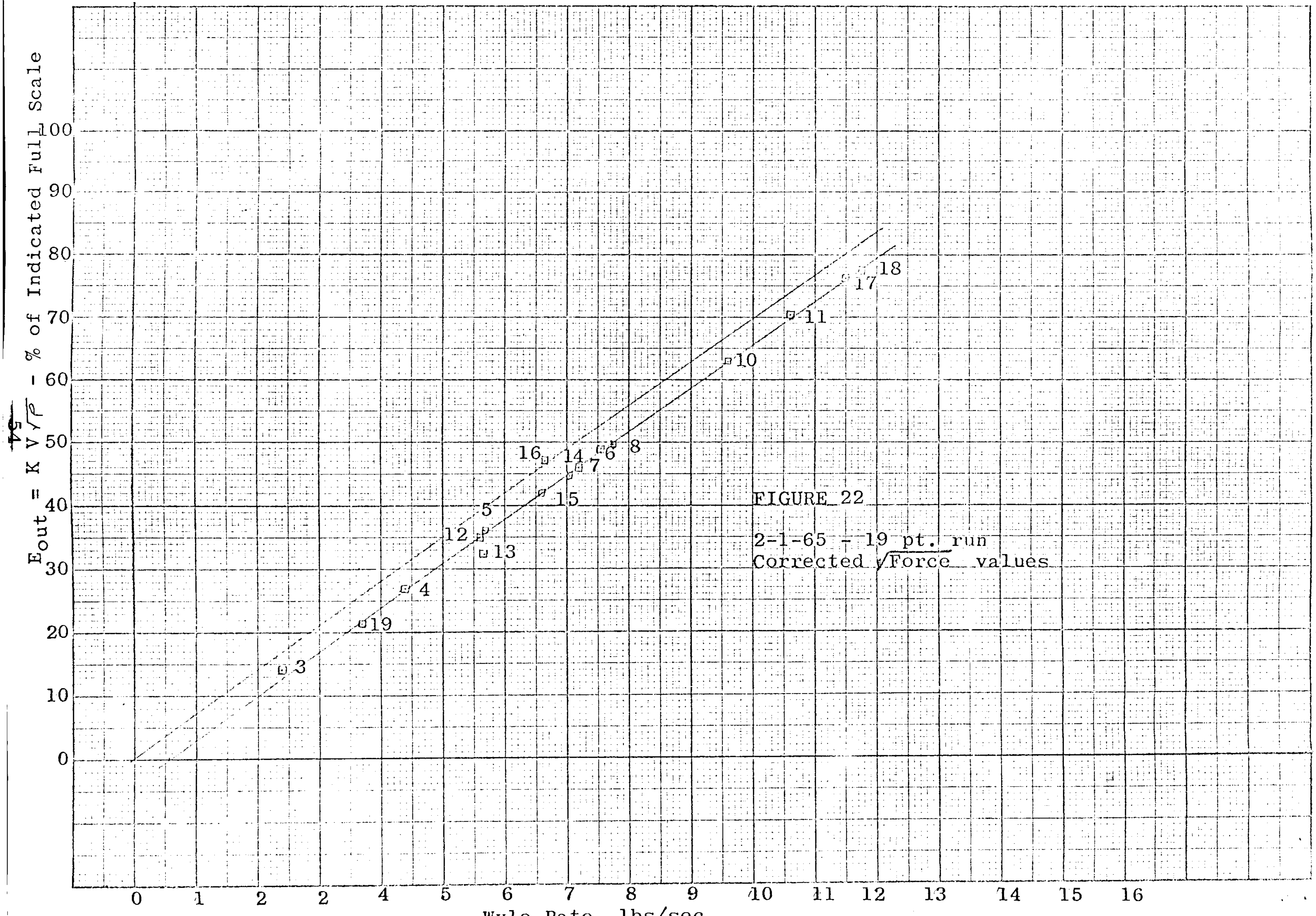
FIGURE 22
2-1-65 - 19 pt. run
Corrected √Force values
E out = K V √ρ - % of Indicated Full Scale
Wyle Rate, lbs/sec
0
10
20
30
40
50
60
70
80
90
100
0 1 2 2 4 5 6 7 8 9 10 11 12 13 14 15 16
3
19
4
13
12
5
15
16
14
7
6
8
10
11
17
18

CONCLUSIONS

The following problems exist in the present design:

1. Excessive cool down (stabilization) time and temperature error.
2. Requires renulling at each cool down.
3. Over sensitive to slight null errors.
4. Overly vulnerable to foreign materials in fluid.

1. The excessive cool down time is caused by excessive overall mass and inadequate thermal transfer between parts. The reduction of the problem is obviously to reduce over-all mass by weight and size reduction whenever possible (also desirable for other reasons). The thermal transfer problem will be reduced by changing surface to mass ratio, surface characteristics, direct conducting paths, and adding radiators and/or shields.

   Temperature error - by minimizing null shift during temperature change by improved symmetry and heat shielding. Piece part tolerances, material grain direction, stress relieving, etc.

   Assembly techniques to maintain and improve final assembled symmetry.

2. Correct by redesigning for properly secured joints by improved joints or reduced stress in joints. Optimize material stress during cool down, warm up, and operation at any temperature within prescribed range.

   Stress relieving of parts and assemblies, and temperature cycling prior to final calibration.

   Materials selection.

3. This caused by too sharp (stiff) mechanical null that becomes stiffest at cold and is determined by the spring rate of the supporting (flexing) members. Adding formed convolutions to the outer supports will improve this as well as reducing the stress at their mounting points. The lever pivot diaphragms should be optimized with respect to diameter and material thickness to provide maximum flexibility when cold and deformed by pressure differential. The magnetic gap may be increased by a decreased lever ratio (now approximately 2:1). The wider gap would decrease the force effect of gap change and decrease magnetic hysteresis error. Reducing the weight of the outer sensitive (moving parts) will permit reduced lever ratio.

4. The density sensing (honeycomb) plates are susceptible to shorting to each other and to ground from foreign material in the fluid. Coating all surfaces of these parts with Kel-F or Teflon would minimize this problem and also an insulation retention problem that could cause a slight shift in total active capacitance.

Filter screens will be added to both ends of the meter to stop any material large and heavy enough to cause physical damage to the honeycombs.

The three pockets for the levers that could also collect residue will be eliminated by having the fulcrum pivot diaphragm flush with the housing bore.

Other pockets (in the channel filler rings) will be eliminated or made self flushing.

The good correlation of the Bendix Indicated Mass Rate of Flow test data from the 15 point calibration on 1-29-65 showing a rate scatter of $\leq 1\%$ of full scale (15 lbs/sec.) about each of two data correlations shows that the basic theory of operation of the flowmeter system is sound. The fact that the two straight lines best correlate the rate data, and the $\sqrt{\text{force}}$ data during nearly constant density runs indicates that some mechanical instability is present. (Post-Wyle states tests show that no magnetic hysteresis or shifts will occur at LH_2 temperatures.)

The mass rate data of 1-29-65 indicates the electronic readout was adequate for the design goal of a mass rate of flow accuracy $\neq$ 1% of full scale.

RECOMMENDATIONS

Modification of the force transducer to achieve a softer (lower spring rate) mechanical null is necessary to obtain a mass rate of flow accuracy of $\pm$ 1% of full scale from the Bendix Capacitance Type Mass Flowmeter System.